Doctoral Dissertation

Development of a novel, simple technology for designing a chimeric metabolic pathway, synthetic metabolic engineering

Xiaoting Ye

January 2013

Graduate School of Engineering

Osaka University

TABLE OF CONTENTS

1. Introduction

1.1 Metabolic engineering

The use of renewable feedstocks as a starting material for the production of a wide range of value-added chemicals, so called "biorefinery", has been one of the most outstanding issues in building of a sustainable society (Rohlin *et al.*, 2001; Stephanopoulos *et al.*, 2007). Considerable research effort has been exerted to improve the economy of current microbial fermentation-based biorefinery processes. The optimization of the metabolic flux of microbial cells by enhancing the expression levels of desired genes and/or by depleting those of undesired ones has emerged as a powerful strategy to improve microbial cells, called as "metabolic engineering" (Stephanopoulos *et al.*, 1993).

In the past few years, metabolic engineering strategies have been widely employed in the production of various non-natural metabolites that are useful biofuels, bulk chemicals and pharmaceuticals. Atsumi *et al.* demonstrated that a series of alcohol can be synthesized from corresponding 2-keto acids which are intermediates of amino acid biosynthesis, by heterologous expression of an enzyme couple of 2-keto-acid

decarboxylase and alcohol dehydrogenase in *Escherichia coli*. The engineered *E. coli* strains are capable of producing higher alcohols including isobutanol, 1-butanol, 2-methyl-1-butanol, 3-methyl-1-butanol and 2-phenylethanol from glucose (Atsumi *et al.*, 2008). Xia *et al.* used metabolically engineered *E. coli* strains to produce native-size recombinant spider silk protein. In their work, a 284.9 kDa recombinant protein of the spider *Nephila clavipes* is produced and spun into a fiber displaying mechanical properties comparable to those of the native silk (Xia *et al.*, 2010).

Thus, metabolic engineering has been demonstrated to be a powerful strategy to produce value-added biomolecules. Nevertheless, these attempts often suffer from flux imbalances as artificially engineered cells typically lack the regulatory mechanisms characteristic of natural metabolism (Kwok, 2010). Atsumi *et al.* transferred an essential set of enzymes derived from *Clostridium acetobutylicum* to *E. coli* for 1-butanol production. However, owning to the imbalanced metabolic flux and existence of branched metabolic pathways, the butanol production was restricted (Atsumi *et al.*, 2008). Additionally, the production of non-natural biomolecules such as biofuels often raises the problem of stress on the cell due to the solvent toxicity.

1.2 Synthetic metabolic engineering

The concept of cell-free bioconversion originated when Eduard Bucher discovered the cell-free metabolism more than 100 years ago. In 1985, Welch and Scopes reconstructed a glycolytic pathway using individually purified yeast enzymes. The reconstructed pathway is capable of converting 1 M (18% [w/v]) glucose to ethanol within 8 h with nearly 100% molar yield (Welch and Scopes, 1985). Zhang *et al.* constructed a synthetic enzymatic pathway for H_2 production from starch and water by using 13 purified enzymes (Zhang *et al.* 2007). In their work, hydrogen yields higher than the theoretical limit (4 H_2 glucose^{-1}) of anaerobic fermentations was obtained and H_2 production can be achieved from starch at a maximum volumetric production rate of approximately 0.5 mM h^{-1}. Nevertheless, little attention has been paid to the practical application of *in vitro* production systems mainly owing to the economical unprofitability of processes involving enzyme purification. Low-cost production of stable biocatalytic modules with high total turn-over number (TTN) value is a crucial issue for the industrialization of enzymatic conversion processes, and thus the employment of highly stable enzymes would be a promising approach for the

preparation of building blocks for *in vitro* synthetic biology projects (Zhang, 2010; Zhang *et al.*, 2010).

Recently, thermophilic enzymes have been increasingly used in bioindustrial processes owing to their extraordinary operational stability at high temperature and denaturant tolerance (Demirjian *et al.*, 2001; Niehaus *et al.*, 1999). Most of these applications utilize recombinant thermostable enzymes that have been expressed in mesophilic hosts. Depending on the type of applications, thermostable enzymes have been prepared to be cell-free (crude, partially purified or homogenous) or cell-associated (Turner *et al.*, 2007). However, to the best of our knowledge, there has been no report on the development of simple methodologies to combine multiple thermostable catalytic modules for constructing *in vitro* metabolic pathways.

In this thesis, the author proposed a novel, simple technology, which was designated as "synthetic metabolic engineering". The basic strategy of synthetic metabolic engineering is assembly of multiple thermo-tolerant biocatalytic modules, to construct *in vitro* artificial pathways for the production of desired products. Recombinant DNA techniques allow the heterologous overproduction of thermophilic enzymes in mesophilic microorganisms (*e.g.*, *E. coli*). The use of recombinant mesophiles having thermophilic enzymes at high temperatures results in the

denaturation of indigenous enzymes and the minimization of unwanted side reactions. Consequently, highly selective thermophilic biocatalytic modules comparable to the purified enzymes can be readily obtained without costly and cumbersome procedures for enzyme purification (Honda *et al.*, 2010; Restiaway *et al.*, 2011). Compared with the conventional metabolic engineering, synthetic metabolic engineering enables us to rationally combine those biocatalytic modules, which makes it possible to construct *in vitro* synthetic metabolic pathways specialized for chemical manufacturing. More importantly, the excellent stability of thermophilic enzymes can mitigate the major disadvantage of *in vitro* enzymatic conversion systems, namely the inability of protein synthesis and renewal. Restiawaty *et al.* constructed an ATP-regenerating system using a heat-treated *E. coli* recombinant strain overproducing thermostable polyphosphate kinase. By coupling this system with a thermostable glycerol kinase, 80 mM of glycerol 3-phosphate could be produced from 100 mM of glycerol with a molar yield of 80% (Restiawaty *et al.*, 2011). Similarly, Honda *et al.* demonstrated an artificial bio-synthetic pathway with ATP regeneration can be constructed and available for the production of 2-deoxyribose 5-phosphate from fructose by using a mixture of six heat-treated *E. coli* recombinant strains overproducing thermophilic enzymes from *Thermus thermophilus* (Honda *et al.*, 2010).

Compared with conventional fermentation processes, synthetic metabolic engineering would offer a number of potential advantages, such as better process flexibility, elimination of tight transcriptional regulation, and easy optimization of production processes by altering enzyme levels. The absence of a culture medium can markedly simplify the isolation and purification of the product of interest. Moreover, the elimination of microbial growth and byproduct formation would allow us to obtain stoichiometrical conversions as well as an ability to perform thermodynamic predictions of production yield.

To construct an artificial synthetic pathway by synthetic metabolic engineering, four key steps are included: 1) appropriate selection of thermostable enzymes; 2) expression in mesophilic hosts (*e.g.*, *E. coli*); 3) preheating of the cell suspension at high temperature (typically at 70°C for 30 min) to disrupt the cell membrane and to inactivate the indigenous host enzymes; and 4) rational combination of those catalytic modules at adequate ratio to achieve the stoichiometrical conversion (Fig. 1.1).

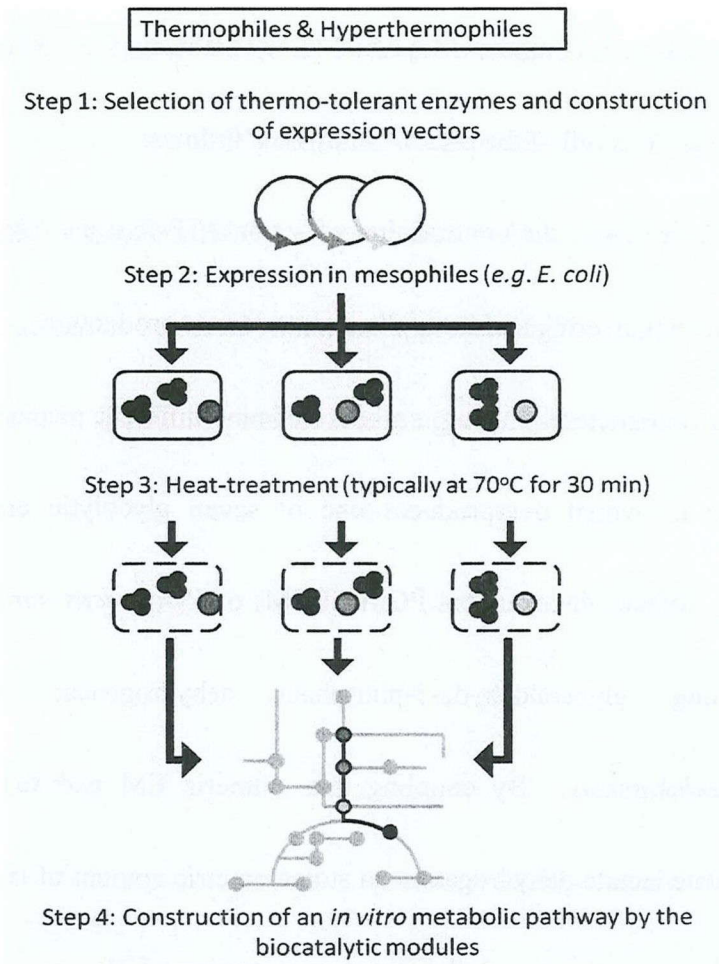

Fig. 1.1 Schematic illustration of the basic procedure of synthetic metabolic engineering.

1.3 Overview of the present study

This thesis proposed a novel and simple technology, designated as "synthetic metabolic engineering" and demonstrated its application to construct a

non-ATP-forming chimeric Embden-Meyerhof (EM) pathway for the production of desired metabolites. Overall of the present study is as follows:

The chapter 2 describes the construction of a non-ATP-forming EM pathway by synthetic metabolic engineering and its application to lactate production. The chimeric EM pathway was constructed by using a mixture of nine different recombinant *E. coli* strains, each one of which overproduces one of seven glycolytic enzymes of *T. thermophilus*, the cofactor-independent PGM (iPGM) of *Pyrococcus horikoshii*, or the non-phosphorylating glyceraldehyde-3-phosphate dehydrogenase (GAPN) of *Thermococcus kodakarensis*. By coupling this chimeric EM pathway with the *T. thermophilus* malate/lactate dehydrogenase, a stoichiometric amount of lactate could be produced from glucose with an overall ATP turnover number of 31.

The chapter 3 deals with malic-enzyme-mediated HCO_3^- fixation by synthetic metabolic engineering. The reversible carboxylation of pyruvate catalyzed by a malic enzyme ($\Delta G^{0'}$= +7.3 kJ mol^{-1}) was coupled with the thermodynamically favorable non-ATP-forming EM pathway to balance the consumption and regeneration of redox cofactors and to shift the overall equilibrium towards malate production (glucose + 2 HCO_3^- + 2 H^+ → 2 malate + 2 H_2O; $\Delta G^{0'}$= -121.4 kJ mol^{-1}). The malic enzyme from *T. kodakarensis* was shown to exhibit both pyruvate carboxylation (pyruvate + HCO_3^- +

NADPH + 2 H^+ → malate + $NADP^+$ + H_2O) and pyruvate reduction (pyruvate + NADPH + H^+ → lactate + $NADP^+$) activities. The reaction specificity of *Tk*ME can be redirected by increasing the HCO_3^- concentration. As a result, direct conversion of glucose to malate can be achieved with a molar yield of 60%.

The conclusions and future prospectives are given in the chapter 4.

2. Construction of a non-ATP-forming Embden-Meyerhof pathway and its application in lactate production

2.1 Introduction

Glycolysis is one of the most universal metabolic pathways and occurs in nearly all organisms. In 1985, Welch and Scopes reconstructed a glycolytic pathway using individually purified yeast enzymes (Welch and Scopes, 1985). Through the reconstructed pathway, 1 M (18% [w/v]) glucose can be converted to ethanol within 8 h with nearly 100% molar yield. In their work, they demonstrated that the imbalance of ATP, which impedes the complete conversion of glucose to ethanol, can be prevented by adding excess amount of arsenate to the reaction mixture. Glyceraldehyde-3-phosphate (GAP) dehydrogenase (GAPDH) can accept arsenate instead of phosphate to form 1-arseno-3-phosphoglycerate, which is simultaneously broken down to arsenate and 3-phosphoglycerate (3-PG). A similar experiment using a cell-free extract of *Zymomonas mobilis* resulted in the conversion of 2 M glucose to 3.6 M ethanol (Algar and Scopes, 1985). The final ethanol concentration (nearly 20%

[v/v]) was higher than any natural fermentation system can achieve, indicating the potential applicability of *in vitro* metabolic system.

As can be seen from Welch and Scope's work, the prevention of cofactor depletion is a critical issue in constructing a synthetic metabolic pathway (Welch and Scopes, 1985). ATP and NAD(P)H are the most important biological phosphate and electron donor, respectively, as they are required for numerous enzymatic reactions in both anabolic and catabolic metabolisms. One of the possible strategies to prevent cofactor depletion is the integration of suitable cofactor-regeneration enzymes into a synthetic pathway. For instance, ATP regeneration systems using thermophilic polyphosphate kinase and polyphosphate have been developed and applied to the production of D-alanyl-D-alanine (Sato *et al.*, 2007) and fructose 1,6-bisphosphate (Iwamoto *et al.*, 2007). Thermophilic $NAD(P)^+$-dependent 6-phosphogluconate dehydrogenase (Wang and Zhang, 2009), glycerol dehydrogenase (Yao and Mikkelsen, 2010), and lactate dehydrogenase (Wichmann and Vasic-Racki, 2005), are available for NAD(P)H regeneration. However, these cofactor-regeneration systems require an exogenous substrate serving as a phosphate and electron donor.

Rapidly expanding genomics and metabolomics information has revealed a great diversity of microbial metabolisms. In fact, although the central metabolic routes of

bacteria and eukaryotes are generally well-conserved, variant pathways consisting of several unique enzymes with unusual cofactor specificities have been developed in archaea (Verhees *et al.*, 2003). For instance, the modified EM pathway of *Pyrococcus furiosus* has only four orthologues of the 10 glycolysis enzymes in bacteria and eukaryotes: triosephosphate isomerase (TIM), phosphoglycerate mutase (PGM), enolase (ENO), and pyruvate kinase (PK) (Dandekar *et al.*, 1999). Glucokinase (GK) and phosphofructokinase (PFK) of *P. furiosus* are ADP-dependent enzymes that are not related to the classical ATP-dependent kinases involved in the bacterial/eukaryotic EM pathway (Kengen *et al.*, 1995; Tuininga *et al.*, 1999). Although the conversion of GAP into 3-PG is catalyzed by the enzyme couple of the NAD^+-dependent GAPDH and the ATP-generating phosphoglycerate kinase (PGK) in the classical EM pathway, the GAP ferredoxin oxidoreductase (GAPOR) is responsible for the single-step phosphate independent conversion of GAP into 3-PG in *P. furiosus* (Mukund and Adams, 1995). A variant enzyme, non-phosphorylating GAPDH (GAPN), that utilizes NAD^+ and/or $NADP^+$ as the cofactor for the phosphate-independent oxidation of GAP has also been found and characterized in several archaeal strains involving *Thermoproteus tenax* (Brunner *et al.*, 1998), *Sulfolobus solfataricus* (Ettema *et al.*, 2007), and *T. kodakarensis* (Matsubara *et al.*, 2011). The substitution of GAPDH and PGK of the classical EM

pathway by archaeal GAPN theoretically enables the construction of a chimeric pathway, in which the consumption and regeneration rates of ATP and ADP are balanced (Fig. 2.1). Moreover, GAPN can bypass the production of the extremely thermolabile intermediate 1,3-bisphosphoglycerate (Ettema *et al.*, 2007). Meanwhile, the glucose oxidation via the chimeric EM pathway yields the reducing equivalents in the form of NAD(P)H. To demonstrate the feasibility of the chimeric EM pathway, a NADH-dependent malate/lactate dehydrogenase was employed to achieve the redox balance of the cofactor and direct conversion from glucose to lactate.

Lactate has been attracting a great attention for its application in food, cosmetic, pharmaceutical and chemical applications (Dumbrepatil *et al.*, 2008). However, in the conventional lactate fermentation process, fermentation broth contains impurities such as color, residual sugars, nutrients, and other organic acids, apart from cell mass (Joglekar *et al.*, 2006). Many studies concerning lactate separation using different techniques such as direct distillation, solvent extraction, adsorption and electrodialysis, have been conducted in order to reduce the operating cost (Kim and Moon, 2001). Synthetic metabolic engineering without the use of a culture medium would markedly simplify the isolation and purification of lactate.

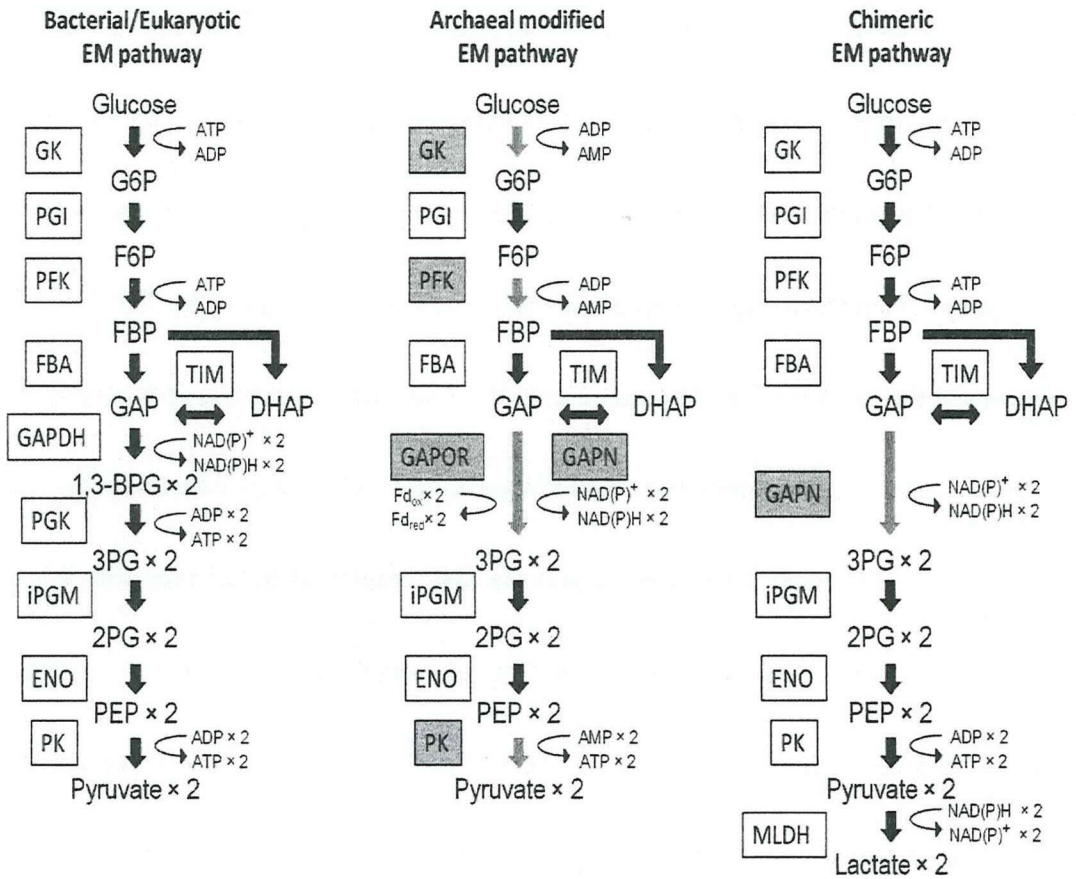

Fig. 2.1 Schematic illustration of design of chimeric Embden-Meyerhof (EM) pathway. The bacterial/eukaryotic classic EM pathway (left), modified EM pathway of *Thermococcales* archaea (center), and chimeric EM pathway constructed in this study (right) are illustrated. Reactions catalyzed by enzymes uniquely involved in the archaeal modified EM pathway are indicated by grey arrows. Abbreviations used: G6P, glucose-6-phosphate; F6P, fructose-6-phosphate; FBP, fructose-1,6-bisphosphate; GAP, glyceraldehyde-3-phosphate; DHAP, dihydroxyacetone phosphate; 1,3-BPG, 1,3-bisphosphoglycerate; 3-PG, 3-phosphoglycerate; 2-PG, 2-phosphoglycerate; PEP, phosphoenolpyruvate; GK, glucose kinase; PGI, glucose-6-phosphate isomerase; PFK, 6-phosphofructokinase; FBA, fructose-bisphosphate aldolase; TIM, triosephosphate isomerase; PGM, phosphoglycerate mutase; ENO, enolase; PK, pyruvate kinase; MLDH, malate/lactate dehydrogenase, GAPOR, glyceraldehyde-3-phosphate ferredoxin oxidoreductase; GAPN, non-phosphorylating glyceraldehyde-3-phosphate dehydrogenase; GAPDH, glyceraldehyde-3-phosphate dehydrogenase; PGK, phosphoglycerate kinase; Fd_{ox}, oxidized ferredoxin; and Fd_{red}, reduced ferredoxin.

2.2 Materials and methods

2.2.1 Bacterial strain and plasmid

The expression vectors for genes encoding GK, PGI, PFK, FBA, TIM, ENO, PK, and MLDH of *T. thermophilus* HB8 were obtained from the Riken *Thermus thermophilus* HB8 expression plasmid set (Yokoyama *et al.*, 2000). The expression vector for GAPN (Matsubara *et al.*, 2011) was a kind gift from Professor H. Atomi of Kyoto University. The gene encoding iPGM was amplified by PCR from the chromosomal DNA of *Pyrococcus horikoshii* OT3 (Takara Bio) with the following primers: 5'-TTCATATGGTGCTAAAGAGGAAAGGC-3' (the *Nde*I restriction site is underlined) and 5'-TTGAATTCTCAAGCTCCAAATTTTTCGCTCCT-3' (the *EcoR*I restriction site is underlined). The amplified DNA was digested with *Nde*I and *EcoR*I and inserted into the corresponding restriction sites of pET21a (Novagen).

E. coli Rossetta2 (DE3) (Novagen) was used as a host strain for gene expression. The recombinants were aerobically cultivated in Luria-Bertani (LB) media containing 100 μg ml^{-1} ampicillin and 34 μg ml^{-1} chloramphenicol at 37°C. Gene expression was induced by an addition of 0.2 mM isopropylthiogalactoside (IPTG) to late-log culture

for 4 h. Cells were harvested by centrifugation and resuspended in 50 mM HEPES-NaOH buffer (pH 7.0). The cell suspensions were heated at 70°C for 30 min before being used for lactate production.

2.2.2 Enzyme assays

E. coli cell suspensions were disrupted with a UD-201 ultrasonicator (Kubota, Osaka, Japan), and the crude lysate was heated at 70°C for 30 min. Cell debris and denatured proteins were removed by centrifugation at 15,000 rpm and 4°C for 10 min. The supernatant was then used as an enzyme solution. Protein concentration was measured with the Bio-Rad assay system (Bio-Rad, Hercules, CA, USA) using bovine serum albumin as the standard.

One unit of the enzyme was defined as the amount consuming 1 μmol of the substrate per min under the assay conditions. The standard assay mixture for GK was composed of 50 mM HEPES-NaOH (pH 7.0), 0.1 mM glucose, 0.2 mM ATP, 5 mM $MgCl_2$, 0.5 mM $MnCl_2$, 1 mM NAD^+, 1 mM G1P, 0.08 U of PGI, 0.2 U of PFK, 1 U of FBA, 0.1 U of TIM, 0.02 U of GAPN, and an appropriate amount of GK. The mixture without glucose was preincubated at 50°C for 2 min, and then the reaction was initiated

by an addition of 0.1 mM glucose. The reduction of NAD^+ was monitored at 340 nm using a UV-VIS spectrophotometer (Model UV-2450, Shimadzu, Kyoto, Japan). Similarly, the activities of PGI, PFK, FBA, TIM, and GAPN were spectrophotometrically assessed in the mixture containing the substrate for each enzyme (0.1 mM of glucose-6-phosphate, fructose-6-phosphate, fructose-1,6-bisphosphate, dihydroxyacetone phosphate, or 0.2 mM GAP, respectively) instead of glucose.

iPGM activity was assayed at 50°C in a mixture consisting of 50 mM HEPES-NaOH (pH 7.0), 0.2 mM 3-phosphoglycerate, 5 mM $MgCl_2$, 0.5 mM $MnCl_2$, 0.2 mM ADP, 0.2 mM NADH, 0.5 U of ENO, 0.5 U of PK, 1.2 U of LDH, and an appropriate amount of enzyme. ENO and PK were assayed in the same manner using 0.2 mM of 2-phosphoglycerate and phosphoenolpyruvate as the substrate, respectively.

The activities of LDH and MLDH were assessed at 50°C by mixing the enzymes with 50 mM HEPES-NaOH (pH 7.0), 5 mM $MgCl_2$, 0.5 mM $MnCl_2$, 0.2 mM NADH, and 0.2 mM pyruvate. NADH oxidation was monitored at 340 nm.

The heat-treated cell lysate of the recombinant *E. coli* harboring an empty vector showed no detectable level of activity under the assay conditions.

2.2.3 Lactate production

The reaction mixture (4 ml) was composed of 0.1 mM glucose, 0.2 mM 3-PG, 0.2 mM pyruvate, 5 mM $MgCl_2$, 0.5 mM $MnCl_2$, 0.2 mM ATP, 0.2 mM ADP, 1 mM NAD^+, 0.2 mM NADH, 1 mM G1P, and 50 mM HEPES-NaOH buffer (pH 7.0). The cell suspensions of *E. coli* producing GK, PGI, PFK, FBA, TIM, GAPN, iPGM, ENO, PK, and MLDH were preheated at 70°C for 30 min and then added into the reaction mixture at final concentrations of 2, 1, 1, 1, 1, 26, 3, 3, 3, and 100 mg (wet weight cells)/ml, respectively. The reaction mixture was stirred in a container kept at 50°C, and glucose solution (40 mM) was added to the mixture at a flow rate of 1 μl min^{-1} (= 0.01 μmol ml^{-1} min^{-1}) using a Shimadzu LC-20AD solvent delivery unit. Aliquots (50 μl) of the reaction mixture were withdrawn at 1 h intervals, diluted fourfold with distilled water, and centrifuged to remove the cell debris (15,000 rpm, 10 min). The supernatant was then ultrafiltered using Amicon 3K (Millipore) and analyzed by a high-performance liquid chromatography (HPLC).

2.2.4 Analytical methods

Lactate and pyruvate were quantified by HPLC on two tandemly connected ion exclusion columns (Shim-pack SPR-H, 250 mm × 7.8 mm, Shimadzu). The columns were eluted at 50°C using 4 mM *p*-toluenesulfonic acid as a mobile phase of at a flow rate of 0.3 ml min^{-1}. The eluent was mixed with a pH-buffered solution (16 mM Bis-Tris, 4 mM *p*-toluenesulfonic acid, and 0.1 mM EDTA) supplied at a flow rate of 0.3 ml min^{-1}, and then analyzed for lactate using a conductivity detector (CDD-20A, Shimadzu, Kyoto, Japan). NAD^+ and NADH concentrations were analyzed colorimetrically using a NAD/NADH quantification kit (Biovision, Mountain View, CA, USA) in accordance with the procedure provided in the kit. ATP and ADP concentrations were assessed quantitatively using the EnzyLight ADP/ATP ratio assay kit (BioAssay Systems, Hayward, CA, USA) according to the manufacturer's instructions.

2.3 Results

2.3.1 Selection of enzymes for chimeric EM pathway

GAPN, a key enzyme for constructing a chimeric EM pathway, was derived from the hyperthermophilic archaeon *T. kodakarensis*. Although both NAD^+ and $NADP^+$ can serve as the electron acceptor, the K_m of *Thermococcus* GAPN for $NADP^+$ is two orders of magnitude lower than that for NAD^+ (Matsubara *et al.*, 2011). However, the thermostability of $NADP^+$ is considerably lower than that of NAD^+, particularly under neutral and acidic conditions (Wu *et al.*, 1986). Owing to this fact, NAD^+ was employed as the redox cofactor for the construction of a chimeric pathway. The enzyme can be strongly activated by the addition of glucose-1-phosphate (G1P) (Matsubara *et al.*, 2011). Under the assay conditions employed in this study, GAPN exhibited the highest specific activity in the presence of G1P at 100 μM or higher.

The thermophilic bacterium *T. thermophilus* HB8 was used as the source of other genes required for the construction of a chimeric pathway. Among them, the cofactor-independent phosphoglycerate mutase (iPGM) showed a relatively low thermal stability (Fig. 2.2). Although the thermal inactivation of other enzymes was insignificant, the activity of the *Thermus* iPGM was lost almost completely after the incubation of the enzymes at 50°C for 2 h. The author then isolated and heterologously expressed the gene encoding iPGM from a hyperthermophilic archaeon, *P. horikoshii*, exhibiting a higher optimum growth temperature (98°C) (González *et al.*,

1998) than that of *T. thermophilus* (70°C) (Oshima and Imahori, 1974). Although the specific activity and thermal stability of the *Pyrococcus* iPGM were not markedly different from those of *Thermus* enzyme, they were considerably improved by the addition of Mn^{2+} (Fig. 2.2). This finding was in good agreement with a previous report that the thermal stability of iPGM from the thermophilic archaeon *Archaeoglobus fulgidus*, which shares a 47.5% amino acid sequence identity with the *Pyrococcus* enzyme, can also be improved by an addition of Mn^{2+} (Johnsen *et al.*, 2007). On the basis of these results, *Pyrococcus* iPGM was employed and used it in the presence of Mn^{2+}.

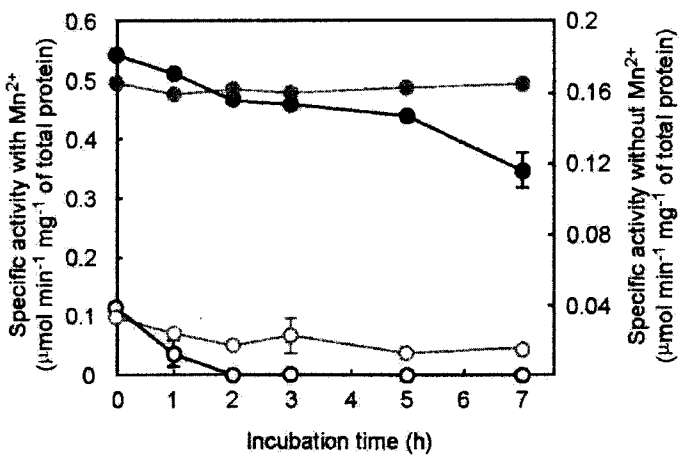

Fig. 2.2 Effects of Mn^{2+} on the activity and thermal stability of the *Pyrococcus* iPGM and *Thermus* iPGM. The crude extract of recombinant *E. coli* with *Pyrococcus* iPGM (grey circle) or *Thermus* iPGM (black circle) was incubated at 50°C in 50 mM HEPES-NaOH (pH 7.0) with (solid circle) or without (empty circle) 0.5 mM $MnCl_2$. The residual iPGM activities were determined under standard assay conditions except that $MnCl_2$ was absent in the assay mixture for the enzyme solutions incubated without $MnCl_2$.

Some bacterial lactate dehydrogenases are inhibited by ATP and/or NAD^+, and thus play an important role in the allosteric regulation of the flux of glycolysis (Garvie, 1980). Although the inhibitory effect of ATP (up to 1 mM) was almost negligible, the addition of 0.1, 0.2, and 1 mM NAD^+ caused 60, 76, and 95% decreases in the activity of *Thermus* lactate dehydrogenase compared with that under the standard assay conditions, respectively (Fig. 2.3). Owing to the low affinity of GAPN to NAD^+, the chimeric pathway, therefore, required a certain amount of exogenous NAD^+. This limitation led the author to search for another enzyme that catalyzes the reduction of pyruvate to lactate. A putative NAD(P)H-dependent dehydrogenase, which was annotated as malate/lactate dehydrogenase (MLDH), was found in the gene-expression library of *T. thermophilus* HB8 (Yokoyama *et al.*, 2000). The enzyme was confirmed to show pyruvate reducing activity with no inhibitory effect by NAD^+ or other metabolic intermediates in this pathway (Fig. 2.3). The natural substrate of this enzyme was unknown and it might more preferably accept metabolite other than pyruvate in physiological conditions. However, the *in vitro* synthetic pathway involves only a limited number of necessary metabolites, and thus an enzyme with broad substrate specificity is also available. More importantly, the allosteric regulation

of the pathway flux can be eliminated by assembling enzymes derived from distinct organisms or metabolic pathways.

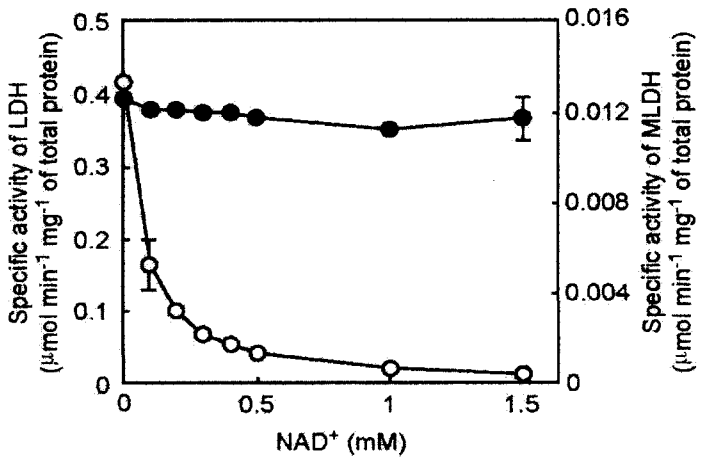

Fig. 2.3 Inhibitory effect of NAD^+ on activities of lactate dehydrogenase (empty circle) and malate/lactate dehydrogenase (solid circle) of *T. thermophilus*. The assay was performed at 50°C in the mixture composed of 50 mM HEPES-NaOH (pH 7.0), 0.2 mM pyruvate, 0.2 mM NADH, an appropriate amount of enzyme, and the indicated concentration of NAD^+. After the preincubation for 2 min at 50°C, the reaction was initiated by an addition of pyruvate.

2.3.2 Optimization of reaction conditions

One of the major advantages of *in vitro* metabolic pathways is the flexibility of the reaction conditions. As long as the enzymes exhibit acceptable activities, reaction conditions can be freely adjusted and optimized. All the enzymes used to construct the chimeric EM pathway exhibited their maximum activity at 60°C or higher (Fig. 2.4A).

However, the degradation of cofactors as well as the thermostabilities of some intermediates of the EM pathway, particularly those of GAP, DHAP, and PEP, became significant at 60°C or higher (Fig. 2.4B). Consequently, the reaction temperature of 50°C was chosen as a compromise between the thermostability of intermediates and enzyme activity. The specific activities of the crude extracts of *E. coli* recombinants harboring each enzyme were assessed at various pH (Table 2.1). On the basis of the pH profiles of each enzyme, the total protein concentrations of the enzyme mixture (containing 0.01 U each of GK, PGI, PFK, FBA, and TIM, along with 0.02 U each of GAPN, iPGM, ENO, PK, and MLDH) was found to be minimized at pH 7.0 (Table 2.1).

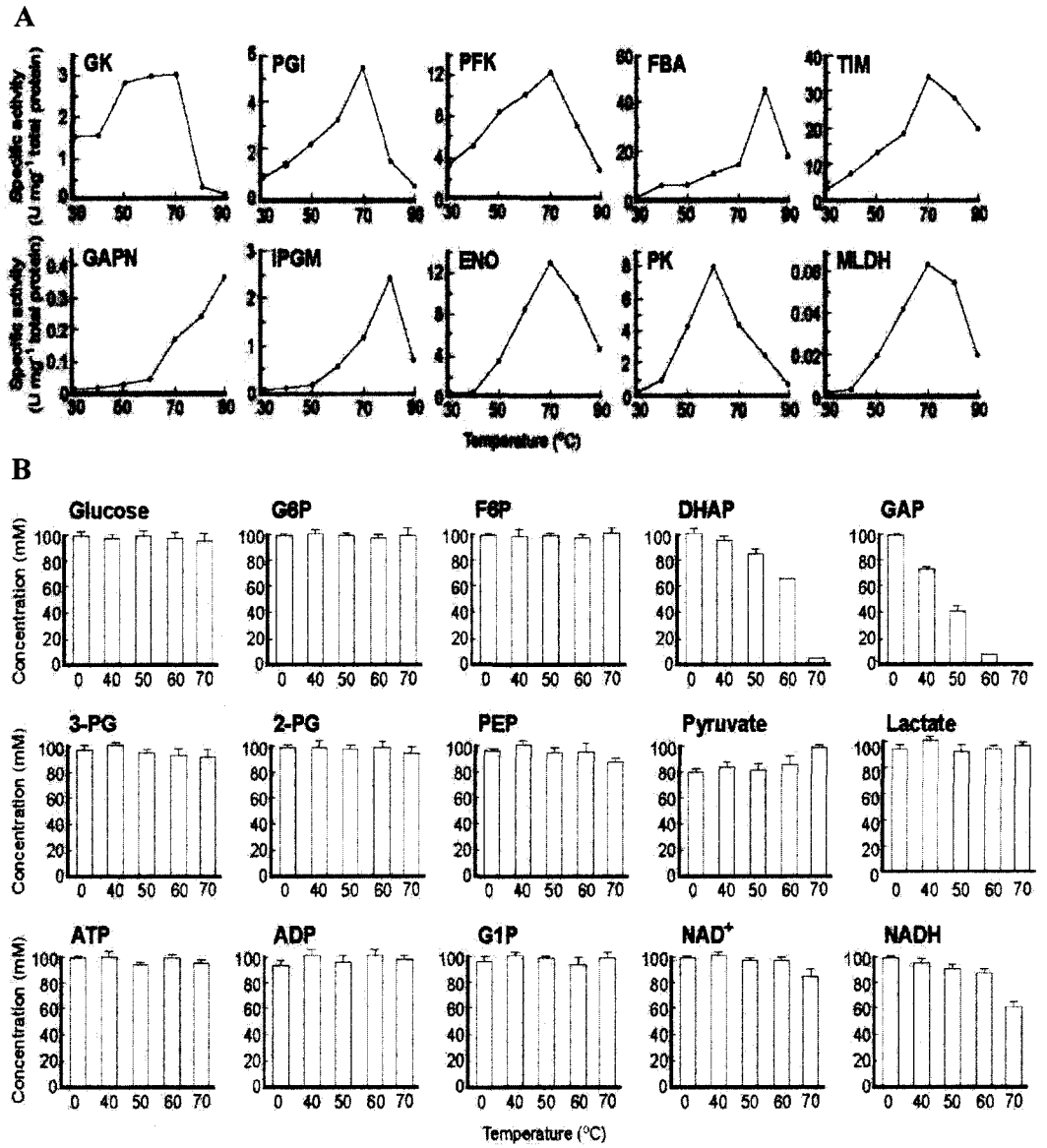

Fig. 2.4 Effects of temperature on enzyme activity and thermal stability of intermediates and cofactors involved in chimeric EM pathway. (A) The enzyme activities were determined under the standard assay conditions (HEPES-NaOH, pH 7.0) at indicated temperatures. Specific activities were given as those in the crude extract of recombinant *E. coli* having each enzyme. One unit was defined as the amount of enzyme catalyzing the consumption of 1 μmole of the substrate per minute. (B) The intermediates and cofactors were dissolved in 50 mM HEPES-NaOH (pH 7.0) and incubated for 1 h at 0, 40, 50, 60, and 70°C. The residual concentration of intermediates was determined by CE-TOFMS (Itoh *et al.*, 2004). ATP, ADP, NAD^+, and NADH (0.1 mM) were determined as described in 2.2.4.

Table 2.1 Effects of pH on enzyme activity

Buffer	pH	Specific activity (U mg^{-1} total protein) [a]										Total protein concentration ($mg\ ml^{-1}$) [b]
		GK	PGI	PFK	FBA	TIM	GAPN	iPGM	ENO	PK	MLDH	
MES	6	0.19	7.6	4.9	7.3	9.2	0.030	0.11	1.1	9.4	0.0026	8.6
MES	7	3.7	7.3	18	7.3	17	0.039	0.17	2.6	5.2	0.013	2.2
HEPES	7	2.9	2.3	8.8	6.9	13	0.036	0.20	3.1	4.5	0.019	1.7
HEPES	8	5.1	11	18	6.5	5.0	0.042	0.087	1.2	0.65	0.014	2.2
Bicine	8	4.5	16	15	4.0	2.1	0.035	0.078	1.3	1.0	0.011	2.7
Bicine	9	7.5	14	18	2.4	0.07	0.041	0.035	0.66	0.42	0.012	3.0
CHES	9	6.0	14	30	4.4	0.9	0.031	0.017	0.40	0.19	0.0095	4.1
CHES	10	2.6	6.1	10	4.6	2.3	0.0051	0.00075	0.10	0.047	0.0021	41

[a] The specific enzyme activities in the crude extract of recombinant *E. coli* were determined under standard assay conditions (50°C) at indicated pHs.

[b] The total protein concentration of the mixture of crude extracts containing the essential enzyme titer (0.01 U each of GK, PGI, PFK, FBA, and TIM, and 0.02 U each of GAPN, iPGM, ENO, PK, and MLDH) was estimated.

2.3.3 Real-time estimation of production rate

For the real-time estimation of production rate, the whole pathway was divided in two parts; 1) the top part (glucose to 3-PG) and 2) the bottom part (3-PG to lactate). The former part, involving GK, PGI, PFK, FBA, TIM, and GAPN, catalyzed the conversion of glucose to 3-PG with concomitant NADH production, which could be spectrophotometrically monitored at 340 nm. On the basis of the enzyme activities, which were individually determined under standard assay conditions, essential units of enzymes (*i.e.*, 0.01 U each of GK, PGI, PFK, FBA, and TIM, and 0.02 U of GAPN) were incubated with 0.1 mM glucose at pH 7.0 and 50°C. The initial NADH production rate observed under these conditions, however, was considerably lower than the expected value of 0.02 μmol ml^{-1} min^{-1}. The expected production rate could be achieved by increasing the units of PFK, FBA and GAPN to 0.2, 1 and 0.03 U, respectively. In the constructed pathway, the actual concentrations of the respective metabolites were kept at lower levels than those used in the standard assay conditions. Consequently, the reaction rates of each enzyme, especially those with relatively high K_m value for their substrates, were lower than those observed under standard assay conditions. Larger amounts of the enzymes were, therefore, required to achieve the

expected production rate. Similarly, the NADH consumption rate of the bottom part (from 3-PG to lactate) was determined with an initial 3-PG concentration of 0.2 mM. The NADH could be consumed at a rate of 0.02 μmol ml^{-1} min^{-1} in the mixture containing 0.02 U each of iPGM, ENO, PK, and MLDH. By this way, the essential amounts of enzymes constituting the top and bottom parts of the synthetic pathway were experimentally determined.

2.3.4 Lactate production by chimeric pathway

All the enzymes employed in this study were heterologously produced in *E. coli* Rosetta2 (DE3) under control of the T7 promoter in the native form with no additional tag sequence. The recombinant cells were suspended in 50 mM HEPES-NaOH buffer (pH 7.0) and preheated at 70°C for 30 min to disrupt the cell membrane and to inactivate *E. coli* enzymes. Lactate production using the chimeric pathway was performed directly using a mixture of heat-treated recombinant cells with the experimentally determined amounts of enzymes to achieve a production rate of 0.02 μmol ml^{-1} min^{-1}. Addition of glucose to the reconstituted pathway at an inadequate dose was suspected to result in an uncontrolled glucose phosphorylation. As excess

glucose feeding causes a rapid glucose phosphorylation by GK, insufficient ATP for the further phosphorylation of F6P catalyzed by PFK would be observed as a result. By contrast, lower feeding rate would result in a decrease in lactate production rate. Thus, unlike the use of living microbial cells, in which glucose uptake rate is regulated by specific glucose transporters (Meadow *et al.*, 1990; Postma *et al.*, 1993), the optimization of substrate feeding rate is necessary for the operation of the reconstituted pathway. As expected, the molar yield of lactate production decreased when the feeding rate exceeded 0.01 μmol ml^{-1} min^{-1} (Fig. 2.5A). The obtained yield which was slightly higher than theoretical yield was likely attributed to an addition of intermediates (0.1 mM glucose, 0.2 mM 3-PG and 0.2 mM pyruvate) into the reaction mixture, performed in order to achieve the constant production rate during the reaction. At a feeding rate of 0.01 μmol ml^{-1} min^{-1}, production rate remained constant at its expected value (0.02 μmol ml^{-1} min^{-1}) during the initial 5 h, and approximately 6 mM of lactate was produced from 3 mM of glucose (Fig. 2.5B, black circle). However, production rate started to decrease after 5 h, and the molar yield of lactate production rapidly dropped to 58% at 10 h (Fig. 2.5B, empty circle). Concurrently, pyruvate accumulation was detected. Whereas the thermal inactivation of all enzymes involved in the chimeric pathway was insignificant after the incubation at 50°C for 10

h, the thermal decomposition of both NAD^+ and NADH, particularly NADH, was not negligible (Fig. 2.5B, squares). The depletion of the cofactor likely caused a decrease in the catalytic performance of MLDH. Moreover, the rate of the GAPN-mediated reaction was particularly sensitive to the depletion of the cofactor owing to its relatively high K_m for NAD^+. A decrease in the rate of the GAPN-mediated reaction led to the accumulation and decomposition of the thermolabile intermediates GAP and DHAP, and to a decrease in the overall lactate production yield. Lactate production rate was recovered by addition of 1 mM NADH after the reaction for 5 h. The final lactate concentration reached 12 mM with an overall production yield of 100% at 10 h. From the actual ATP and ADP concentrations of the reaction mixture (0.4 mM), the ATP turnover number was calculated to be 31. The ATP turnover number was defined as moles of the product formed per moles of the cofactor added. The effect of cell-derived endogenous ATP and ADP (0.37 μM) was considered to be negligible.

A

Time	Total glucose (mM)	Lactate (mM)	Yield (%)
Feeding rate = 0.04 μmol ml^{-1} min^{-1}			
1	2.4	1.54 ±0.31	32.2
2	4.8	1.59 ±0.52	16.6
Feeding rate = 0.02 μmol ml^{-1} min^{-1}			
1	1.2	2.17 ±0.53	90.5
2	2.4	3.22 ±0.08	67.2
Feeding rate = 0.01 μmol ml^{-1} min^{-1}			
1	0.6	1.45 ±0.23	121
2	1.2	2.48 ±0.26	103

B

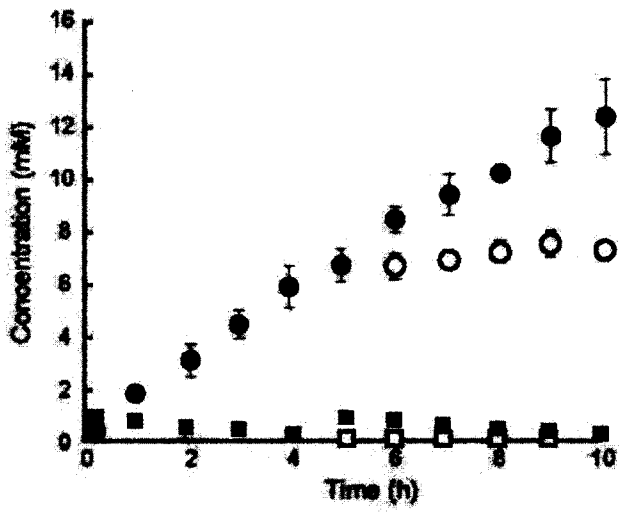

Fig. 2.5 Lactate production via chimeric EM pathway. (A) The lactate production was performed as described in Materials and methods with glucose feeding at indicated rates. After the reaction for 1 and 2 h, lactate concentration was determined by HPLC, and yield on glucose (% mol/mol) was calculated. (B) Time course of lactate production at a glucose feeding rate of 0.01 μmol ml^{-1} min^{-1} (circle). The total concentration of NAD^+ and NADH are indicated by square symbols. Lactate and NAD(H) concentrations with or without an additional NADH supplement (1 mM) after the initial 5-h reaction are shown by solid and empty symbols, respectively.

2.4 Discussion

In this work, a glycolytic pathway with no net ATP yield was constructed by chimerically integrating the archaeal GAPN to a classical EM pathway. The synthetic pathway produced a stoichiometric amount of lactate from glucose with an overall ATP turnover number of 31. Note that such a non-ATP-forming glycolysis pathway could no longer play a physiological role (*i.e.*, energy production particularly under anaerobic conditions) and thus would not be applicable for a fermentative purpose *in vivo*. In fact, although the GAPDH defect of *E. coli* can be complemented with the *Pisum sativum* GAPN under aerobic condition, this recombinant strain fails to grow anaerobically (Valverde *et al.*, 1999).

Although the author demonstrated that the endogenous ATP regeneration could be achieved, the thermolability of NADH remained a major obstacle for the long-term operation of a synthetic metabolic system. A possible alternative to overcome this limitation is the replacement of NADH with more stable and low-cost artificial biomimetic NADH analogs (Ansell and Lowe, 1999). Protein engineering approaches to improve the affinities of enzymes to these NADH biomimics may be also required (Ryan *et al.*, 2008). Another important issue that should be resolved is

the increase in production rate. Although it was predicted to increase proportionally along with a total enzyme concentration (Tuesink *et al.*, 2000), the total amount of enzymes required to obtain a desired rate is often not practically achievable. On the other hand, naturally occurring cellular apparatus, in which a series of metabolic enzymes are packed in close proximity, can reduce the intermediate diffusion distance and therefore increase the overall reaction rate. The coexpression of thermophilic enzymes constituting a synthetic pathway in a single recombinant will be an effective strategy to spatially organize the enzymes and achieve a high production rate (Conrado *et al.*, 2008).

2.5 Summary

A chimeric EM pathway was constructed by synthetic metabolic engineering using a mixture of nine different recombinant of *E. coli* strains, each one of which overproduces either one of seven glycolytic enzymes of *T. thermophilus*, the iPGM of *P. horikoshii*, or the GAPN of *T. kodakarensis*. By coupling this chimeric EM pathway with the *T. thermophilus* malate/lactate dehydrogenase, a stoichiometric

amount of lactate could be produced from glucose with an overall ATP turnover number of 31.

3. Direct conversion of glucose to malate by synthetic metabolic engineering

3.1 Introduction

With the threat of global climate change, there is a growing demand for techniques of converting CO_2 into renewable fuels and chemicals (Atsumi *et al.*, 2009; Li *et al.*, 2012). The applicability of biocatalysts to the conversion of CO_2 to aspartate, isocitrate, and formate has been demonstrated over the past few decades (Parkinson and Weaver, 1984; Ruschig *et al.*, 1976; Melzer and O'Leary, 1987). CO_2 reduction mediated by a malic enzyme, which can catalyze the reversible carboxylation of pyruvate to malate with the concomitant oxidation of NAD(P)H to $NAD(P)^+$ has been examined more extensively in recent years as a promising approach to greenhouse gas fixation and the production of useful biocommodities (Ohno *et al.*, 2008; Zheng *et al.*, 2009).

Malate, which is a potential biomass-derivable "building block" for chemical synthesis, has been widely used in food, cosmetic, pharmaceutical, and chemical applications (Chibata *et al.*, 1983; Zelle *et al.*, 2008). In 2004, the US Department of

Energy included a group of 1,4-dicarboxylic acids, consisting of succinate, fumarate, and malate, in the top 12 most interesting chemical building blocks that can be derived from biomass (Werpy and Petersen, 2004).

The use of a malic enzyme can provide a shortcut for C_4-dicarboxylic acid production. Ohno *et al.* reported the fixation of HCO_3^- to pyruvate using a purified malic enzyme from *Pseudomonas diminuta* coupled with glucose 6-phosphate and glucose 6-phosphate dehydrogenase for NADH regeneration. The system is capable of converting 100 mM pyruvate to 38 mM L-malate within 24 h with a 38% molar yield (Ohno *et al.*, 2008). A similar experiment using a purified malic enzyme of *Brevundimonas diminuta* conjugated with the electrochemical regeneration of NADH on an enzyme-mediator-immobilized electrode, resulted in a nearly 1.1 mmol of malate production from 12.5 mmol of pyruvate and 2.5 mmol of $NaHCO_3$ within 48 h (Zheng *et al.*, 2009).

It is crucial to determine the thermodynamical feasibility of carboxylation reactions. According to the second law of thermodynamics, such reactions occur only in the direction of the negative Gibbs energy of reaction. The oxidative formation of malate catalyzed by a malic enzyme (pyruvate + HCO_3^- + NADPH + 2 H^+ → malate + $NADP^+$ + H_2O; $\Delta G^{0'} = +7.3$ kJ mol^{-1}) is thermodynamically unfavorable (Thauer *et al.*,

1977; Goldberg *et al.*, 1993). One of the possible strategies to solve this problem is coupling with thermodynamically favorable NAD(P)H regeneration enzymes including glucose 1-dehydrogenase (glucose + $NADP^+$ → glucono-1,5-lactone + NADPH + H^+; $\Delta G^{0'}$ = -4.0 kJ mol^{-1}), glucose 6-phosphate dehydrogenase (glucose-6-phosphate + $NADP^+$ → glucono-1,5-lactone 5-phosphate + NADPH + H^+; $\Delta G^{0'}$ = -9.3 kJ mol^{-1}), and 6-phosphogluconate dehydrogenase (6-phosphogluconate + $NADP^+$ → ribulose-5-phosphate + CO_2 + NADPH + H^+; $\Delta G^{0'}$ = -43.6 kJ mol^{-1}). In the chapter 2, an *in vitro* thermodynamically favorable non-ATP-forming EM pathway using a mixture of nine different recombinant *E. coli* strains has been constructed (glucose + 2 $NAD(P)^+$ → 2 pyruvate + 2 NAD(P)H + 2 H^+, $\Delta G^{0'}$= -136.4 kJ mol^{-1}). In this pathway, GAPN, which utilizes NAD^+ or $NADP^+$ as cofactors for the phosphate-independent oxidation of GAP, was employed as a substitute for GAPDH and ATP-generating PGK. Thus, the regeneration and consumption rates of ATP and ADP could be balanced (Ye *et al.*, 2012). Moreover, the glucose oxidation via the chimeric EM pathway yields the reducing equivalent in the form of NAD(P)H. The inability of ATP formation via the chimeric EM pathway leads to a larger negative $\Delta G^{0'}$ of approximately -136 kJ mol^{-1} than that via the classical EM pathway, which theoretically enables the shift in the equilibrium of malic-enzyme-mediated carboxylation.

In this chapter, the author aimed to demonstrate the thermodynamical feasibility of the chimeric EM pathway for redirecting reversible carboxylation, which is catalyzed by a NAD(P)H-dependent malic enzyme derived from the hyperthermophilic archaeon *T. kodakarensis* (*Tk*ME), to achieve the direct conversion of glucose to malate (glucose + 2 HCO_3^- + 2 H^+ → 2 malate + 2 H_2O; $\Delta G^{0'}$ = -121.4 kJ mol^{-1}) (Fig. 3.1).

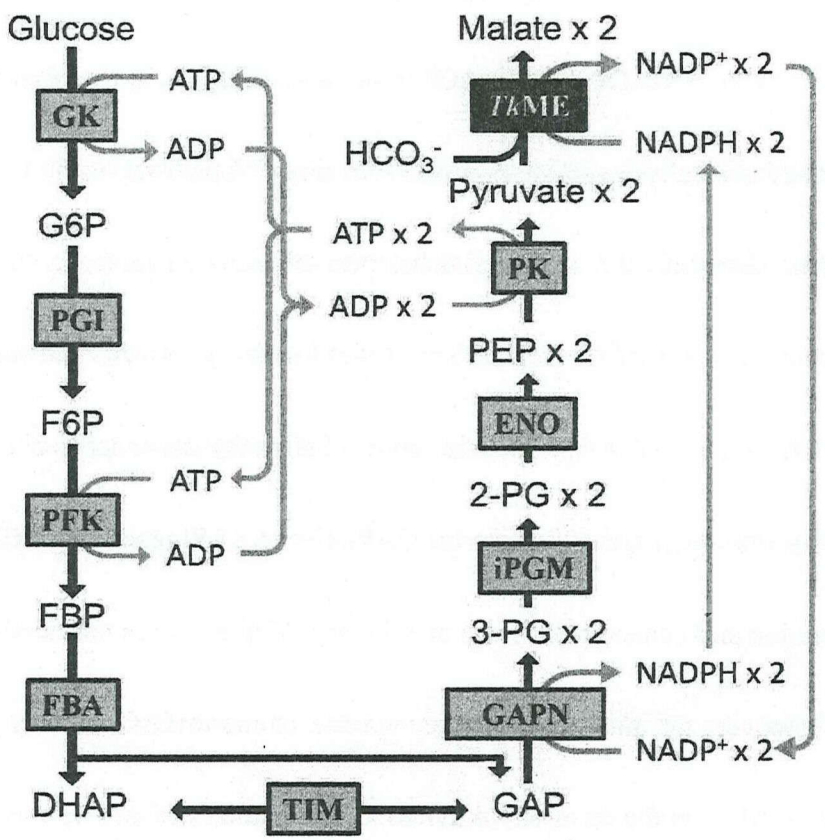

Fig. 3.1 Schematic illustration of design of synthetic pathway for direct conversion of glucose to malate. ME, malic enzyme.

3.2 Materials and methods

3.2.1 Plasmid construction and protein expression

The gene encoding *Tk*ME was amplified by PCR from the chromosomal DNA of *T. kodakarensis* KOD1 (Takara Bio, Shinga, Japan) using the following primers: 5'-TTCATATGAATCCCCTCGAATTCCATAGGGA-3' (the *Nde*I restriction site is underlined) and 5'-TTAAGCTTCTAGGGGGAACTCCCTCTACCG-3' (the *Hind*III restriction site is underlined). The amplified DNA was digested with *Nde*I and *Hind*III and inserted into the corresponding restriction sites of pET21(a) (Novagen, Madison, WI, USA). The resulting expression vector was transformed into *E. coli* Rosseta2 (DE3) (Novagen). The expression vectors for glucokinase (GK), glucose-6-phosphate isomerase (PGI), 6-phosphofructokinase (PFK), fructose-bisphosphate aldolase (FBA), triosephosphate isomerase (TIM), enolase (ENO), and pyruvate kinase (PK) of *T. thermophilus*, iPGM of *P. horikoshii*, and GAPN of *T. kodakarensis* were described previously (Ye *et al.*, 2012).

The recombinants were aerobically cultivated in Luria-Bertani (LB) medium containing 100 μg ml^{-1} ampicillin and 34 μg ml^{-1} chloramphenicol at 37°C. Gene

expression was induced by adding 0.2 mM IPTG to late-log culture for 4 h. Cells were harvested by centrifugation and resuspended in 50 mM HEPES-NaOH buffer (pH 7.0). The cell suspensions were heated for 30 min at 70°C and then used for malate production.

3.2.2 Malic enzyme assay

E. coli cells were disrupted with a UD-201 ultrasonicator (Kubota, Osaka, Japan), and the crude lysate was heated at 70°C for 30 min. Cell debris and denatured proteins were removed by centrifugation at 12,000 × *g* and 4°C for 10 min. The supernatant was then used as the enzyme solution. Protein concentration was measured with the Bio-Rad assay system (Bio-Rad, Hercules, CA, USA) using bovine serum albumin as the standard. One unit of the enzyme was defined as the amount consuming 1 μmol of the substrate per minute under the assay conditions.

The pyruvate carboxylation activity (malate-forming) of *Tk*ME was determined by monitoring the decrease in NADPH concentration at 340 nm using a UV-VIS spectrophotometer (Model UV-2450, Shimadzu, Kyoto, Japan) at 50°C. The standard reaction mixture was composed of 500 mM HEPES-NaOH buffer (pH 7.0), 10 mM

NH_4Cl, 0.5 mM $MnCl_2$, 0.2 mM NADPH, 15 mM pyruvate, 80 mM $NaHCO_3$, and an appropriate amount of enzyme. The optimum HCO_3^- concentration for *Tk*ME was determined at 50°C. The pyruvate reduction activity (lactate-forming) was subtracted from each measurement. Pyruvate reduction activity was measured similarly at 50°C except that the reaction mixture contained no $NaHCO_3$ and the reaction was initiated by adding 15 mM pyruvate.

3.2.3 Determination of carboxylating species

The active carboxylating species was spectrophotometrically determined by a modified method (Erb *et al.*, 2009) at 15°C, monitoring the rate of NADPH oxidation at 340 nm. All the solutions were prepared freshly and stored on ice before use. The carboxylation with "dissolved CO_2" was measured in a reaction mixture (0.1 ml) containing 500 mM HEPES-NaOH (pH 7.0), 10 mM NH_4Cl, 0.5 mM $MnCl_2$, 0.2 mM NADPH, 15 mM pyruvate, and an appropriate amount of enzyme. To start the carboxylation, 1.5 µl of 1 M $NaHCO_3$ was mixed with 9 µl of 1 M acetic acid to generate CO_2 from bicarbonate by acidification, and this "CO_2 solution" was added to reaction mixture immediately. A "bicarbonate" solution was prepared by mixing 1.5

μl of 1 M $NaHCO_3$ with 9 μl of H_2O and added to the reaction mixture immediately. As control experiments, both reactions were performed with an appropriate amount of human erythrocyte carbonic anhydrase (Sigma-Aldrich, St. Louis, Missouri, USA).

3.2.4 Malate production coupled with glucose 1-dehydrogenase at various HCO_3^- concentrations

The standard reaction mixture contained 500 mM HEPES-NaOH (pH 7.0), 10 mM NH_4Cl, 0.5 mM $MnCl_2$, 1 mM NADPH, 1 mM pyruvate, 1 mM glucose, 0.3 U of glucose 1-dehydrogenase (GDH; Thermostable Enzyme Laboratory, Kobe, Japan), and an appropriate amount of *Tk*ME. The initial concentrations of $NaHCO_3$ added were 0, 21.3, 42.5, and 85 mM. The reaction mixture was stirred in a sealed container kept at 50°C, and the headspace of the container was equilibrated with a N_2 gas mixture containing 0, 25, or 50% CO_2 gas or with 100% of CO_2 gas for 5 min before the addition of substrates. After the reaction for 5 h at 50°C, the mixture was ultrafiltered using Amicon 3K (Millipore) and subjected to high-performance liquid chromatography (HPLC).

3.2.5 Production of malate from glucose

The preparation of heat-treated cell suspensions was described in chapter 2 (Ye *et al.*, 2012). Cell suspensions of *E. coli* producing GK, PGI, PFK, FBA, TIM, GAPN, iPGM, ENO, PK, and *Tk*ME were added to the reaction mixture at final concentrations of 1, 1, 1, 1, 1, 2, 5, 5, 5, and 5 mg (wet cell weight)/ml, respectively. The reaction mixture (4 ml) also contained 0.1 mM glucose, 0.2 mM 3-phosphoglycerate, 1 mM pyruvate, 5 mM $MgCl_2$, 0.5 mM $MnCl_2$, 10 mM NH_4Cl, 0.2 mM ATP, 0.2 mM ADP, 1 mM $NADP^+$, 1 mM NADPH, 1 mM glucose 1-phosphate, 80 mM $NaHCO_3$, and 500 mM HEPES-NaOH buffer (pH 7.0).

The reaction mixture was stirred in a 10-ml rubber-capped reaction vessel. The mixture was equilibrated with 100% CO_2 gas for 5 min at 50°C before the addition of the substrates. Then the vessel was further sealed with Parafilm M (Pechiney Plastic Packaging, Chicago, USA) to prevent CO_2 leakage and the mixture of 40 mM glucose and 80 mM $NaHCO_3$ solutions was added to the reaction mixture at a flow rate of 1 μl min^{-1}(= 0.01 μmol ml^{-1} min^{-1} glucose and 0.02 μmol ml^{-1} min^{-1} $NaHCO_3$) using a Shimadzu LC-20AD solvent delivery unit. The mixture of glucose and $NaHCO_3$ solutions was equilibrated with 100% CO_2 gas throughout the reaction. Aliquots (50

μl) of the reaction mixture were drawn, diluted fourfold with ice-chilled water, and centrifuged to remove cell debris (15,000 rpm, 10 min, 4°C). The supernatant was then ultrafiltered using Amicon 3K (Millipore) and subjected to HPLC. $NADP^+$ and NADPH concentrations were analyzed colorimetrically using a NADP/NADPH quantification kit (Biovision, Mountain View, CA, USA) in accordance with the procedure provided in the kit. Pyruvate, malate, and lactate were quantified by HPLC on two tandemly connected ion exclusion columns (Shim-pack SPR-H, 250 mm × 7.8 mm, Shimadzu) as described in the chapter 2.

3.3 Results

3.3.1 Characterization of recombinant TkME

Although *Tk*ME can accept both $NADP^+$ and NAD^+ as electron acceptors for the oxidative decarboxylation of malate, its activity with NAD^+ was seven times lower than that with $NADP^+$ (Fukuda *et al.*, 2005). Thus, NADP(H) was employed as the redox cofactor for the construction of the chimeric pathway. In malate decarboxylation, recombinant *Tk*ME showed the highest activity at pH 8 above 90°C

(data not shown). These results were in good agreement with the previous results (Fukuda *et al.*, 2005). In the pyruvate carboxylation reaction, the optimal pH and temperature were 6.5 and 70°C (Figs. 3.2A and 3.2B). Although the enzyme was derived from the hyperthermophilic archaeon *T. kodakarensis*, whose optimum growth temperature was approximately 85°C (Atomi *et al.*, 2004), the optimum temperature for the carboxylation activity of *Tk*ME was much lower (70°C). This was likely attributed to the decrease in the saturation concentration of CO_2 at high temperatures. In addition to the oxidative decarboxylation of malate and the reductive carboxylation of pyruvate, *Tk*ME was found to have a pyruvate reduction activity (the reduction of pyruvate to lactate). The pH profile of the pyruvate reduction activity was similar to that of the pyruvate carboxylation activity; the highest pyruvate reduction activity was observed above 90°C probably owing to its independence of CO_2 concentration (Figs. 3.2B and 3.2D). Several studies have shown that malic enzymes from various sources can catalyze the reduction of pyruvate to lactate (Yamaguchi, 1979; Tang and Hsu, 1973). However, the physiological role of the archaeal malic enzyme remains unclear. Our finding may give insight into the precise function of malic enzymes in the unique metabolism of hyperthermophilic archaea.

Some malic enzymes are activated by NH_4^+ and K^+ (Kawai *et al.*, 1996; Gourdon

et al., 2000). This was also shown to be the case for *Tk*ME. The addition of NH_4^+ (10 mM) could markedly increase the carboxylation activity of *Tk*ME by 16.1-fold (Table 3-1). On the other hand, activation of *Tk*ME by the addition of K^+ was modest, and no synergistic effect of NH_4^+ and K^+ was observed. Thus, we employed 10 mM of NH_4^+ in malate production.

Table 3-1

Effects of NH_4^+ and K^+ concentrations on *Tk*ME activity

		NH_4^+ (mM)		
		0	5	10
K^+ (mM)	0	100	1150	1610
	5	540	1530	1600
	10	740	1500	1690

Assays were performed under the standard conditions with indicated concentrations of NH_4^+ and K^+.
Activities were expressed as percentages of that observed in the absence of NH_4^+ and K^+.

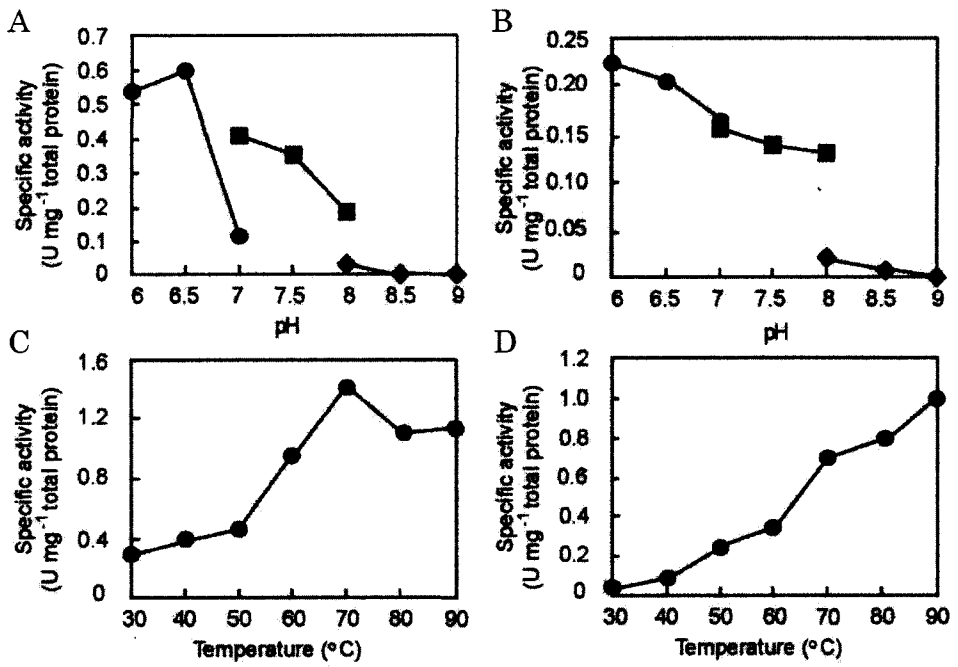

Fig. 3.2 Effects of pH (A, B) and temperature (C, D) on pyruvate carboxylation (A, C) and pyruvate reduction (B, D) activities of *Tk*ME. One unit was defined as the amount of enzyme catalyzing the consumption of 1 μmol of the substrate per minute. MES-NaOH (circles), HEPES-NaOH (squares), and Bicine-NaOH (diamonds) were used to adjust pH.

3.3.2 Determination of active carboxylating species

The identification of the active species for *Tk*ME-mediated carboxylation is crucial to decide the reaction conditions for malate production via the synthetic pathway. Although Dalziel and Londesborough (1968) demonstrated that the malic enzyme from wheat germ preferably accepts dissolved CO_2 as the carboxylation species, Asami *et al.* (1979) reported that HCO_3^- serves as the substrate for pyruvate

carboxylation catalyzed by the maize malic enzyme. To identify the active carboxylating species for *Tk*ME, NADPH oxidation in the mixture consisting of pyruvate and *Tk*ME was spectrophotometrically determined at 340 nm upon the addition of either dissolved CO_2 or HCO_3^- at 15°C. Below 20°C, the interconversion of HCO_3^- and CO_2 takes more than 1 min; therefore, the effect of dissolved CO_2 and HCO_3^- on the initial carboxylation rate can be determined (Erb *et al.*, 2009). As shown in Fig. 3.3, the initial reaction rate with HCO_3^- as the substrate was higher than that with CO_2, suggesting that HCO_3^- served as the carboxylating species for *Tk*ME. As control, both reactions were performed in the presence of carbonic anhydrase. Carbonic anhydrase, which catalyzes the reversible interconversion of CO_2 and HCO_3^-, accelerates the equilibration between them. As expected, similar NADPH oxidation rates were observed in the presence of carbonic anhydrase in both reactions. The initial rate of carboxylation was dose-dependently increased by increasing HCO_3^- concentration until 100 mM (Fig. 3.4).

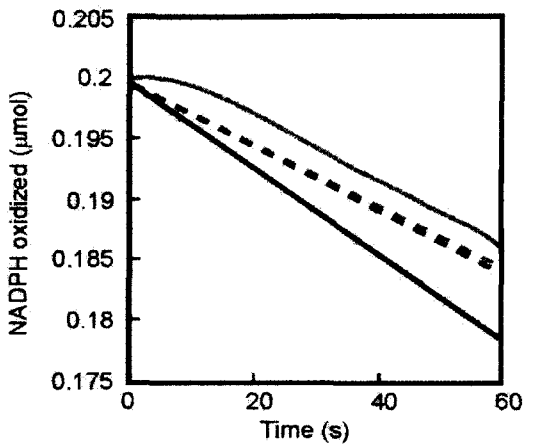

Fig. 3.3 Determination of carboxylating species of *Tk*ME-mediated malate production. NADPH oxidation was spectrophotometrically determined at 340 nm at 15°C. To determine the carboxylating species, the reaction was started with either dissolved CO_2 (grey solid line), or HCO_3^- (black solid line) at 15°C, at which CO_2 hydration/HCO_3^- dehydration is slow. As control experiments, the reaction was performed in the presence of carbonic anhydrase with dissolved CO_2 (grey dotted line) or HCO_3^- (black dotted line).

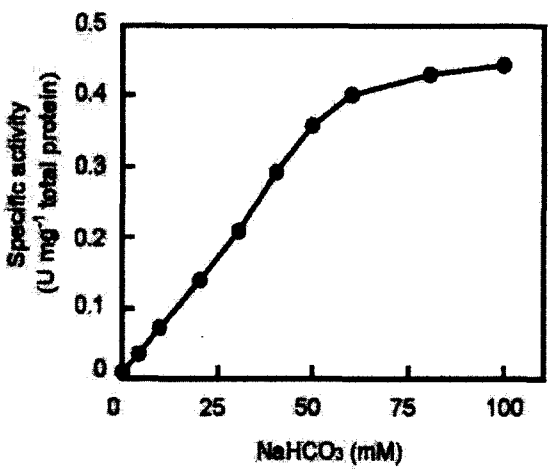

Fig. 3.4 Effect of HCO_3^- concentration on initial rate of *Tk*ME-mediated carboxylation. The reaction rate with 15 mM pyruvate was monitored at different HCO_3^- concentration. Buffer strength was set to 0.5 M to minimize the pH shift caused by HCO_3^- addition.

3.3.3 *Effect of HCO_3^- concentration on reaction specificity*

Pyruvate carboxylation catalyzed by *Tk*ME was accompanied by lactate formation and the carboxylation rate of *Tk*ME was shown to be dose-dependent on the HCO_3^- concentration in the solution phase (Fig. 3.4). At given pHs and temperatures, the HCO_3^- concentration in the solution phase is proportional to the partial pressure of CO_2 (Umbreit *et al.*, 1957), and the equilibrated HCO_3^- concentration was calculated to be 85 mM at 50°C, pH 7 and a CO_2 partial pressure of 1 atm (see Appendix).

To determine the effect of HCO_3^- concentration on malate production, the reactions were performed in the reaction mixtures containing 0, 21.3, 42.5, and 85 mM HCO_3^-, which were equilibrated with N_2 gas mixtures containing 0, 25, and 50% CO_2 and with 100% CO_2, respectively. Buffer strength was set to 0.5 M to minimize the pH shift caused by HCO_3^- addition.

The author observed that the addition of equimolar amounts of the substrate and cofactor (pyruvate and NADPH) failed to produce detectable amounts of malate probably owing to the thermodynamically unfavorable manner of carboxylation (data not shown). Therefore, carboxylation was carried out using *Tk*ME coupled with GDH to regenerate the coenzyme and to shift the overall chemical equilibrium.

Besides, HCO_3^- concentration was varied to investigate their effects on the reaction specificity of *Tk*ME, as well as to shift the equilibrium. As expected, the formation of lactate was largely prevented by increasing HCO_3^- concentration, which consequently improved malate production (Fig. 3.5). The highest malate concentration of 0.62 mM was obtained when 85 mM HCO_3^- was added to the reaction mixture at a CO_2 pressure of 1 atm.

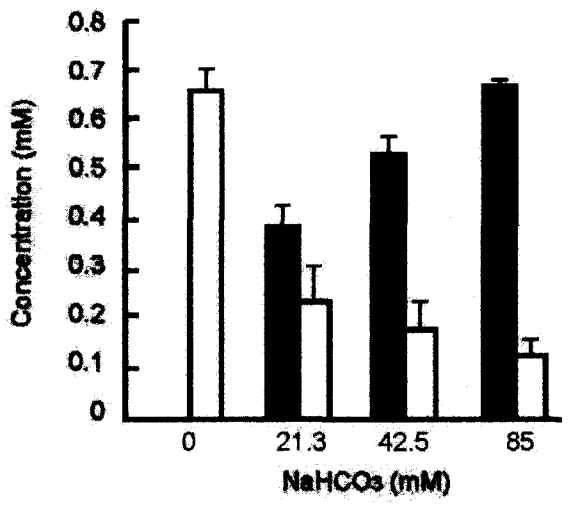

Fig. 3.5 Effect of HCO_3^- on reaction specificity. The assay was performed at 50°C for 5 h, and lactate (white bar) and malate (black bar) were quantified. The reaction mixture was composed of 500 mM HEPES-NaOH (pH 7.0), 10 mM NH_4Cl, 0.5 mM $MnCl_2$, 1 mM NADPH, 1 mM pyruvate, 1 mM glucose, 0.3 U of GDH , 0.1 U of *Tk*ME, and the indicated concentration of HCO_3^-.

3.3.4 Direct conversion of glucose to malate through synthetic pathway

Malate production was performed at 50°C using a mixture of heat-treated

recombinant cells with experimentally determined amounts of enzymes to achieve a production rate of 0.02 μmol ml^{-1} min^{-1}. The essential amounts of enzymes required to achieve the expected production rates were optimized as described in chapter 2 (Ye *et al*, 2012). *Tk*ME activity was spectrophotometrically assessed, and the enzyme amount to give a malate production rate of 0.02 μmol ml^{-1} min^{-1} was determined. An initial pyruvate concentration of 1 mM was employed owing to its relatively high K_m value for pyruvate (Fukuda *et al.*, 2005). Production rate remained constant during the initial 2 h. Approximately 2.6 mM malate and 0.6 mM lactate were produced from 1.8 mM glucose within 3 h and the malate yield was calculated to be 72%. After 4-h reaction, the molar yield of malate dropped down to 60% (Fig. 3.6). We confirmed that the recombinant *Tk*ME was fully stable at 50°C for 10 h. Besides, we had observed that the conversion rate of glucose through the chimeric EM pathway was constant in the presence of a certain level of cofactors (Ye *et al.*, 2012). This observation indicates that the thermal inactivation of the enzymes involved in the chimeric EM pathway was insignificant for at least 10 h at 50°C. Similarly, the author confirmed that the degradation of ATP and ADP was insignificant at 50°C (Ye *et al.*, 2012). However, the thermal decomposition of both $NADP^+$ and NADPH was not negligible (Fig. 6). It seems likely to have caused a decrease in the catalytic

performance of GAPN and *Tk*ME. ATP turnover number was calculated to be 9 from the actual ATP and ADP concentrations of the reaction mixture (0.4 mM). ATP turnover number was defined as number of moles of the product formed per mole of the cofactor added.

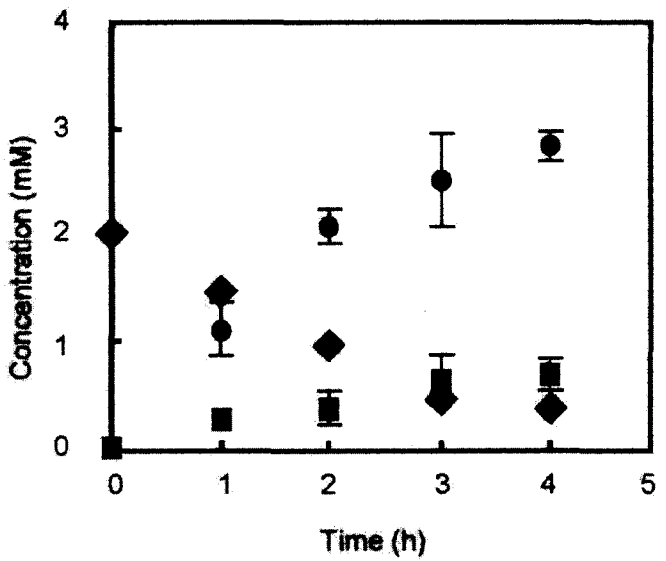

Fig. 3.6 Time course of malate production through synthetic pathway. Malate production was performed as described in the text at a glucose feeding rate of 0.01 μmol ml^{-1} min^{-1} and a HCO_3^- feeding rate of 0.02 μmol ml^{-1} min^{-1}. The malate, lactate, and NADP(H) concentrations are indicated by circles, squares, and diamonds, respectively.

3.4 Discussion

In this chapter, the author constructed a synthetic pathway, by coupling the non-ATP-forming chimeric EM pathway with the malic-enzyme-mediated HCO_3^-

fixation into pyruvate, for the direct conversion of glucose to malate (glucose + 2 HCO_3^- + 2 H^+ → 2 malate + 2 H_2O; $\Delta G^{0'}$= -121.4 kJ mol^{-1}). Despite the thermodynamical unfavorability of pyruvate carboxylation catalyzed by the malic enzyme ($\Delta G^{0'}$= +7.3 kJ mol^{-1}), the coupling with the non-ATP-forming chimeric EM pathway successfully shifted the overall chemical equilibrium towards malate production. *Tk*ME was found to exhibit both pyruvate carboxylation (malate-forming) and pyruvate reduction (lactate-forming) activities; the reaction specificity could be shifted to obtain malate as the primary product by increasing HCO_3^- concentration.

From the viewpoint of practical applications, the utilization of CO_2 in malate production is more desirable than that of HCO_3^-. Thus, the direct fixation of CO_2 into pyruvate was attempted by sparging CO_2 gas into the reaction mixture containing *Tk*ME and GDH at 50°C. However, the system produced only 0-1 mM malate from 100 mM pyruvate. This was probably due to the lower saturation concentration of CO_2 at higher temperatures (Mook *et al.*, 1974) and to the lower hydration rates of CO_2 (CO_2 + H_2O → H_2CO_3) (Dalziel and Londesborough, 1968). To increase the hydration rate, the integration of a thermophilic carbonic anhydrase, which can catalyze the interconversion between CO_2 and H_2CO_3, would be a promising approach

and is currently under investigation.

Zelle *et al.* reported four natural metabolic pathways for the production of malate from glucose: i) The first is the carboxylation of pyruvate to oxaloacetate, followed by the reduction of oxaloacetate to malate. If pyruvate is produced through glycolysis, this pathway involves the net fixation of CO_2, resulting in a maximum theoretical malate yield of 2 mol (mol glucose)$^{-1}$. ii) The second is the condensation of oxaloacetate and acetyl-coenzyme A (acetyl-CoA) to citrate, followed by its oxidation to malate via the tricarboxylic acid (TCA) cycle. If acetyl-CoA is generated by pyruvate dehydrogenase, the conversion of glucose to malate via this oxidative pathway results in the release of two molecules of CO_2, thus limiting the maximum theoretical malate yield to 1 mol (mol glucose)$^{-1}$. iii) The third is the formation of malate from two molecules of acetyl-CoA via the glyoxylate cycle. In this alternative oxidative pathway for malate production, the maximum malate yield on glucose is limited to 1 mol mol^{-1} owing to the oxidative decarboxylation required for acetyl-CoA production from pyruvate. iv) The fourth is a noncyclic pathway involving glyoxylate cycle enzymes, in which oxaloacetate is replenished by pyruvate carboxylation. The theoretical maximum malate yield on glucose via this pathway is 1.33 mol mol^{-1} (Zelle *et al.*, 2008). Compared with these four natural metabolic

pathways, our chimeric pathway illustrated in Fig. 3.1 can provide a theoretical maximum yield of 2 mol of malate per mol of glucose, which is comparable to the oxaloacetate-mediated malate production. Note that such a direct conversion can hardly be achieved *in vivo* owing to the less favorable conditions for carboxylation, *i.e.*, low intracellular HCO_3^- concentration, which lead to the thermodynamic unfavorability of malic-enzyme-mediated carboxylation. In fact, although the inability of the pyruvate-carboxylase-deficient mutant of *Saccharomyces cerevisiae* to utilize glucose as the sole carbon source could be complemented with a cytosolic-relocalized malic enzyme under CO_2 atmosphere, the growth rates of the strains are considerably lower than that of the wild-type strain (Zelle *et al.*, 2011).

Another important issue that should be resolved is that *Tk*ME shows preference for NADP(H) over NAD(H) as the cofactor (Fukuda *et al.*, 2005). The thermostability of NADP(H) is considerably lower than that of NAD(H) under neutral and acidic conditions (Wu *et al.*, 1986). The rapid degradation of NADPH at high temperatures has restricted the application of NADPH-dependent dehydrogenases. The alteration of the coenzyme specificity of *Tk*ME would be an effective strategy to overcome this limitation and achieve the long-term operation of a synthetic metabolic system. However, the thermal lability of redox cofactors poses a simple question about the

underlying mechanisms by which thermophiles and hyperthermophiles can solve the problem. Further studies aimed at elucidating such mechanisms will be required not only for the deeper understanding of the physiology of (hyper)thermophiles but also for improving the practical applicability of synthetic metabolic engineering.

3.5 Summary

In this chapter, a synthetic pathway for the direct conversion of glucose to malate was constructed. The reversible carboxylation of pyruvate catalyzed by a malic enzyme derived from *T. kodakarensis* was coupled with a thermodynamic favorable non-ATP-forming EM pathway to achieve redox balance and to shift the overall equilibrium towards malate production. *Tk*ME was shown to exhibit both pyruvate carboxylation and pyruvate reduction activities. By increasing the concentration of the substrate of HCO_3^-, the reaction specificity could be redirected to malate production. As a result, the direct conversion of glucose to malate can be achieved with a molar yield of 60%.

3.6 Appendix: calculated concentrations of CO_2, HCO_3^- and CO_3^{2-} at 50°C and a CO_2 partial pressure of 1 atm.

The partitioning of carbon dioxide between the gas and liquid phases is dependent on water pH, since carbon dioxide is buffered in water by the bicarbonate buffer system:

$$CO_2\ (g) \rightarrow CO_2\ (aq)$$

$$CO_2\ (aq) + H_2O \leftrightarrow H_2CO_3$$

Henry's law describes the solubility of an ideal gas in the liquid phase. The solubility of the gas in the liquid phase is proportional to the pressure of the gas over the solution, given as

$$P_{CO2} = K_H \times [H_2CO_3] \qquad (1)$$

where K_H is Henry's constant (expressed on a mole fraction basis), P_{CO2} is the partial pressure of the gas (MPa), and $[H_2CO_3]$ includes dissolved CO_2 and hydrated CO_2 in the liquid phase. However, the dehydration is kinetically slow and only a small fraction (approximately 0.2-1%) of dissolved CO_2 is actually converted to H_2CO_3 at equilibrium. Most of the CO_2 remains as solvated molecular CO_2.

$$K = \frac{[H_2CO_3]}{[CO_2](aq)} \approx 1.7 \times 10^{-3} \qquad (2)$$

Thus,

$$P_{CO_2} = K_H \times [CO_2\ (aq)] \qquad (3)$$

According to Carroll *et al.*, at low pressures (up to 10 atm), Henry's constant could be expressed as,

$$\ln(K_H) = -6.83 + 1.28 \times 10^4/T - 3.77 \times 10^6/T^2 + 3.00 \times 10^8/T^3 \qquad (4)$$

where T is the temperature (K). According to eq. (4), the solubility of CO_2 at 50°C

(323 K) and 1 atm (0.1 MPa) can be calculated to be 19.8 mM.
Carbonic acid is a weak acid that dissociates in two steps.

Step 1. $H_2CO_3\,(aq) \leftrightarrow H^+ + HCO_3^-$

$$K_{a1} = \frac{a[HCO_3^-]}{[H_2CO_3]} = 4.2 \times 10^{-7} \quad (5)$$

Step 2. $HCO_3^- \leftrightarrow H^+ + CO_3^{2-}$

$$K_{a2} = \frac{a[CO3^{2-}]}{[HCO3^-]} = 4.8 \times 10^{-11} \quad (6)$$

where $a = [H^+]$.
The substitution of eq. (6) into eq. (5) yields

$$[CO_2\,(aq)] = [H_2CO_3] = \frac{a^2[CO3^{2-}]}{K_{a1}K_{a2}} \quad (7)$$

Assuming that the initial concentration of carbonic acid = c, then we can derive the stoichiometric relation,

$$c = [H_2CO_3] + [HCO_3^-] + [CO_3^{2-}]. \quad (8)$$

Substituting this into the stoichiometric relations, we derive,

$$[CO_3^{2-}] = \frac{K_{a1}K_{a2}\cdot c}{a^2 + K_{a1}a + K_{a1}K_{a2}}, \quad (9)$$

$$[HCO_3^-] = \frac{K_{a1}a\cdot c}{a^2 + K_{a1}a + K_{a1}K_{a2}}, \quad (10)$$

$$[CO_2\,(aq)] = [H_2CO_3] = \frac{a^2\cdot c}{a^2 + K_{a1}a + K_{a1}K_{a2}}, \quad (11)$$

Assuming a temperature of 50°C and a pressure of 1 atm, the CO_2 concentration in water is calculated to be 19.8 mM. Thus, according to eq. (11), HCO_3^- concentration can be calculated as follows.

pH	CO_2 (mM)	HCO_3^- (mM)	CO_3^{2-} (mM)
1	19.8	8.51×10^{-5}	4.09×10^{-14}
2	19.8	8.51×10^{-4}	4.09×10^{-12}
3	19.8	8.51×10^{-3}	4.09×10^{-10}
4	19.8	8.51×10^{-2}	4.09×10^{-8}
5	19.8	8.51×10^{-1}	4.09×10^{-6}
6	19.8	8.51	4.09×10^{-4}
7	19.8	8.51×10^{1}	4.09×10^{-2}
8	19.8	8.51×10^{2}	4.09
9	19.8	8.51×10^{3}	4.09×10^{2}
10	19.8	8.51×10^{4}	4.09×10^{4}
11	19.8	8.51×10^{5}	4.09×10^{6}
12	19.8	8.51×10^{6}	4.09×10^{8}
13	19.8	8.51×10^{7}	4.09×10^{10}
14	19.8	8.51×10^{8}	4.09×10^{12}

4. Conclusions

Metabolic engineering has become a practical alternative to conventional chemical conversion particularly for biocommodity production processes; however, this approach is often hampered by as yet unidentified inherent mechanisms of natural metabolism. One of the current research directions in the field of metabolic engineering is to gain a deeper understanding of these underlying regulatory networks by exploiting the information obtained from a variety of "-omics" analyses (Itoh *et al.*, 2004). By contrast, synthetic metabolic engineering provides a completely different means to overcome this limitation by reconstituting only the pathway of interest using thermo-tolerant biocatalytic modules. Besides, this approach has several advantageous, such as better process flexibility, ease of optimization of production processes by altering enzyme level. Moreover, the elimination of microbial growth and byproduct formation enables us to achieve stoichiometrical conversion and perform thermodynamic predictions of production yield. In the case no thermophilic enzymes are found, several evolutional approaches can be applied to increase the thermostability of less stable enzymes (Miyazaki *et al.*, 2000; Wintrode *et al.*, 2001). In fact, enzymes can be readily evolved for higher thermostability, owing to the fact

that relatively few amino acid substitutions (1-5% of the sequence) can improve the thermal stability of a mesophilic enzyme (Farinas *et al.*, 2001). In the present study, the author successfully constructed a non-ATP-forming EM pathway by synthetic metabolic engineering and demonstrated its applicability for the production of desired metabolite. The results described in each chapter can be summarized as follows:

Chapter 2 describes the construction of a non-ATP-forming EM pathway and its applicability in the production of lactate. To be specific, a chimeric EM pathway with balanced consumption and regeneration of ATP and ADP was constructed *in vitro* by using nine recombinant *E. coli* strains, each one of which overproduces either one of the seven glycolytic enzymes of *T. thermophilus*, the cofactor-independent phosphoglycerate mutase of *P. horikoshii*, or the non-phosphorylating glyceraldehyde-3-phosphate dehydrogenase of *T. kodakarensis*. To demonstrate the feasibility of the chimeric EM pathway, a NADH-dependent malate/lactate dehydrogenase was employed to achieve the redox balance of the cofactor and direct conversion of glucose to lactate. As a result, 6 mM glucose could be converted to 12 mM lactate within 10 h with nearly 100% molar yield.

Chapter 3 deals with the construction of a synthetic pathway capable of direct conversion of glucose to malate. Reversible carboxylation of pyruvate catalyzed by a

malic enzyme ($\Delta G^{0'}$= +7.3 kJ mol^{-1}) was coupled with the above-mentioned thermodynamically favorable non-ATP-forming EM pathway to balance the consumption and regeneration of redox cofactors and to shift the overall equilibrium towards malate production (glucose + 2 HCO_3^- + 2 H^+ → 2 malate + 2 H_2O; $\Delta G^{0'}$= -121.4 kJ mol^{-1}). Additionally, the author found that the *Tk*ME had both pyruvate carboxylation (malate-forming) and pyruvate reduction (lactate-forming) activities. By increasing the concentration of the substrate of HCO_3^-, the reaction specificity could be redirected to the malate production. As a result, direct conversion of glucose to malate can be achieved with a molar yield of 60%.

The concept of *in vitro* synthetic-pathway biotransformation is not new but its feasibility in practical application has been largely restricted mainly owing to the prejudice that *in vitro* biotransformation is too costly for producing low-value biocommodities. However, the comparative cost analysis between *in vitro* and *in vivo* fermentation processes demonstrated that this interpretation is not necessarily true and that the development of stable standardized enzyme modules will provide economical advantageous to the use of *in vitro* system. Weight-based turnover number (TTN_W) in terms of kg of product per kg of biocatalyst, has been used to compare microbial fermentation and cell-free bioconversion. Typical TTN_W values for intracellular

recombinant protein production by microbial fermentations range from 0.005 to 0.25 (*i.e.*, 1~50% cellular protein is the target recombinant protein and total cellular proteins account for ~50% of cellular weight) (Zhang *et al.*, 2010). Although we have not quantified the total concentration of thermophilic enzymes used in our study, it could be roughly estimated to be around 6 and 5 in the production of malate and lactate, respectively (we estimated it on the basis of the presumption that the recombinant thermophilic enzymes occupy 5% of the total protein of *E. coli*, in average). Therefore, the performance of our system is far more effective than *in vivo* fermentation processes. Meanwhile, since the performance of the *in vitro* enzymatic conversion is independent of the metabolic activity of the cells, highly reproducible reaction rates can be achieved at different reaction scales without complex process controls (Restiawaty *et al.*, 2011).

Synthetic metabolic engineering enables a one-step preparation of highly selective and stable biocatalytic modules via a simple heat-treatment of the recombinant mesophiles having thermophilic enzymes. Most importantly, it is, in principle, applicable to all thermophilic enzymes, as long as they can be functionally expressed in the host, and thus would be potentially applicable to the biocatalytic manufacture of any chemicals or materials on demand.

REFERENCES

Algar, E.M., Scopes, R.K., 1985. Studies on cell-free metabolism: Ethanol production by extracts of *Zymomonas mobilis*. Journal of Biotechnology 2, 275-287.

Ansell, R.J., Lowe, C.R., 1999. Artificial redox coenzymes: Biomimetic analogues of NAD^+. Applied Microbiology and Biotechnology 51, 703-710.

Asami, S., Inoue, K., Matsumoto, K., Murachi, A., Akazawa, T., 1979. NADP-malic enzyme from maize leaf: Purification and properties. Archives of Biochemistry and Biophysics 194, 503-510.

Atomi, H., Fukui, T., Kanai, T., Morikawa, M., Imanaka, T., 2004. Description of *Thermococcus kodakaraensis* sp. nov., a well studied hyperthermophilic archaeon previously reported as *Pyrococcus* sp. KOD1. Archaea 1, 263-267.

Atsumi, S., Higashide, W., Liao, J.C., 2009. Direct photosynthetic recycling of carbon dioxide to isobutyraldehyde. Nature Biotechnology 27, 1177-1180.

Atsumi, S., Cann, A.F., Connor, M.R., Shen, C.R., Smith, K.M., Brynildsen, M.P., Chou, K.J., Hanai, T., Liao, J.C., 2008. Metabolic engineering of *Escherichia coli* for 1-butanol production. Metabolic Engineering 10, 305-311.

Brunner, N.A., Brinkmann, H., Siebers, B., Hensel, R., 1998. NAD^+-dependent glyceraldehyde-3-phosphate dehydrogenase from *Thermoproteus tenax*. The first identified archaeal member of the aldehyde dehydrogenase superfamily is a glycolytic enzyme with unusual regulatory properties. The Journal of Biological Chemistry 273, 6149-6156.

Carroll, J.J., Slupsky, J.D., Mather, A.E., 1991. The solubility of carbon dioxide in water at low pressure. Journal of Physical Chemistry 20, 1201-1209.

Chibata, I., Tosa, T., Takata, I., 1983. Continuous production of L-malic acid by immobilized cells. Trends in Biotechnology 1, 9-11.

Conrado,. R.J., Varner, J.D., DeLisa, M.P., 2008. Engineering the spatial organization of metabolic enzymes: mimicking nature's synergy. Current Opinion in

Biotechnology 19, 492-499.

Dalziel, K., Londesborough, J.C., 1968. The mechanisms of reductive carboxylation reactions. Carbon dioxide or bicarbonate as substrate of nicotinamide-adenine dinucleotide phosphate-linked isocitrate dehydrogenase and malic enzyme. Biochemical Journal 110, 223-230.

Dandekar, T., Schuster, S., Snel, B., Huynen, M., Bork, P., 1999. Pathway alignment: application to the comparative analysis of glycolytic enzymes. Biochemical Journal 343, 115-124.

Demirjian, D.C., Morís-Varas, F., Cassidy, C.S., 2001. Enzymes from extremophiles. Current Opinion in Chemical Biology 5, 144-151.

Ettema, T.J., Ahmed, H., Geerling, A.C., van der Oost, J., Siebers, B., 2007. The non-phosphorylating glyceraldehyde-3-phosphate dehydrogenase (GAPN) of *Sulfolobus solfataricus*: a key-enzyme of the semi-phosphorylative branch of the Entner-Doudoroff pathway. Extremophiles 12, 75-88.

Erb, T.J., Brecht, V., Fuchs, G., Müller, M., Alber, B.E., 2009. Carboxylation mechanism and stereochemistry of crotonyl-CoA carboxylase/reductase, a carboxylating enoyl-thioester reductase. Proceedings of the National Academy of Sciences 106, 8871-8876.

Farinas, E.T., Bulter, T., Arnold, F.H., 2001. Directed enzyme evolution. Current Opinion in Biotechnology 12, 545-551.

Fukuda, W, Ismail, Y.S., Fukui, T., Atomi, H., Imanaka, T., 2005. Characterization of an archaeal malic enzyme from the hyperthermophilic archaeon *Thermococcus kodakarensis* KOD1. Archaea 1, 293-301.

Garvie, E.I., 1980. Bacterial lactate dehydrogenases. Microbiological Review 44, 106-139.

Goldberg, R.N., Tewari, Y.B., Bell, D., Fazio, K., Anderson, E., 1993. Thermodynamics of enzyme-catalyzed reactions: Part 1. Oxidoreductases. Journal

of Physical and Chemical Reference Data 22, 515-579.

González, J.M., Masuchi, Y., Robb, F.T., Ammerman, J.W., Maeder, D.L., Yanagibayashi, M., Tamaoka, J., Kato, C., 1998. *Pyrococcus horikoshii* sp. nov., a hyperthermophilic archaeon isolated from a hydrothermal vent at the Okinawa Trough. Extremophiles 2, 123-130.

Gourdon, P., Baucher, M.F., Lindley, N.D., Guyonvarch, A., 2000. Cloning of the malic enzyme gene from *Corynebacterium glutamicum* and role of the enzyme in lactate metabolism. Applied and Environmental Microbiology 66, 2981-2987.

Hodgman, C.E., Jewett, M.C., 2012. Cell-free synthetic biology: thinking outside the cell. Metabolic Engineering 14, 261-269.

Honda, K., Maya, S., Omasa, T., Hirota, R., Kuroda, A., Ohtake, H., 2010. Production of 2-deoxyribose 5-phosphate from fructose to demonstrate a potential of artificial bio-synthetic pathway using thermophilic enzymes. Journal of Biotechnology 148, 204-207.

Itoh, A., Ohashi, Y., Soga, T., Mori, H., Nishioka, T., Tomita, M., 2004. Application of capillary electrophoresis-mass spectrometry to synthetic *in vitro* glycolysis studies. Electrophoresis 25, 1996-2002.

Iwamoto, S., Motomura, K., Shinoda, Y., Urata, M., Kato, J., Takiguchi, N., Ohtake, H., Hirota, R., Kuroda, A., 2007. Use of an *Escherichia coli* recombinant producing thermostable polyphosphate kinase as an ATP regenerator to produce fructose 1,6-diphosphate. Applied and Environmental Microbiology 73, 5676-5678.

Johnsen, U., Schönheit, P., 2007. Characterization of cofactor-dependent and cofactor-independent phosphoglycerate mutases from Archaea. Extremophiles 11, 647-657.

Kawai, S., Suzuki, H., Yamamoto, K., Inui, M., Yukawa, H., Kumagai, H., 1996. Purification and characterization of a malic enzyme from the ruminal bacterium *Streptococcus bovis* ATCC 15352 and cloning and sequencing of its gene. Applied

and Environmental Microbiology 62, 2692-2700.

Kengen, S.W.M., Tuininga, J.E., de Bok, F.A.M., Stams, A.J.M., de Vos, W.M., 1995. Purification and characterization of a novel ADP-dependent glucokinase from the hyperthermophilic archaeon *Pyrococcus furiosus*. The Journal of Biological Chemistry 270, 30453-30457.

Kwok, R., 2010. Five hard truths for synthetic biology. Nature 463, 288-290.

Lee, J.W., Kim, T.Y., Jang, Y.S., Choi, S., Lee, S.Y., 2011. Systems metabolic engineering for chemicals and materials. Trends in Biotechnology 29, 370-378.

Lee, S.Y., Park, J.H., Jang, S.H., Nielsen, L.K., Kim, J., Jung, K.S., 2008. Fermentative butanol production. Biotechnology Bioengineering 101, 209-228.

Li, H., Opgenorth, P.H., Wernick, D.G., Rogers, S., Wu, T.Y., Higashide, W., Malati, P., Huo, Y.X., Cho, K.M., Liao, J.C., 2012. Integrated electromicrobial conversion of CO_2 to higher alcohols. Science 335, 1596.

Matsubara, K., Yokooji, Y., Atomi, H., Imanaka, T., 2011. Biochemical and genetic characterization of the three metabolic routes in *Thermococcus kodakarensis* linking glyceraldehyde 3-phosphate and 3-phosphoglycerate. Molecular Microbiology 81, 1300-1312.

Meadow, N.D., Fox, D.K., Roseman, S., 1990. The bacterial phosphoenolpyruvate: glycose phosphotransferase system. The Annual Review of Biochemistry 59, 497-542.

Melzer, E., O'Leary, M.H., 1987. Anapleurotic CO_2 fixation by phosphoenolpyruvate carboxylase in C3 plants. Plant Physiology 84, 58-60.

Miyazaki, K., Wintrode, P.L., Grayling, R.A., Rubingh, D.N., Arnold, F.H., 2000. Directed evolution study of temperature adaption in a psychrophilic enzyme. Journal of Molecular Biology 297, 1015-1026.

Mook, W.G., Bommerson, J.C., Staverman, W.H., 1974. Carbon isotope fractionation

between dissolved bicarbonate and gaseous carbon dioxide. Earth and Planetary Science Letters 22, 169-176.

Mukund, S., Adams, M.W., 1995. Glyceraldehyde-3-phosphate ferredoxin oxidoreductase, a novel tungsten-containing enzyme with a potential glycolytic role in the hyperthermophilic archaeon *Pyrococcus furiosus*. The Journal of Biological Chemistry 270, 8389-8392.

Niehaus, F., Bertoldo, C., Kähler, M., Antranikian, G., 1999. Extremophiles as a source of novel enzymes for industrial application. Applied Microbiology and Biotechnology 51, 711-729.

Ohno, Y., Nakamori, T., Zheng, H., Suye, S., 2008. Reverse reaction of malic enzyme for HCO_3^- fixation into pyruvic acid to synthesize L-malic acid with enzymatic coenzyme regeneration. Bioscience Biotechnology Biochemistry 72, 1278-1282.

Oshima, T., Imahori, K., 1974. Description of *Thermus thermophilus* (Yoshida and Oshima) comb. nov., a nonsporulating thermophilic bacterium from a Japanese

Thermal Spa. International Journal of Systematic Bacteriology 24, 102-112.

Parkinson, B.A., Weaver, P.F., 1984. Photoelectrochemical pumping of enzymatic CO_2 reduction. Nature 309, 148-149.

Postma, P.W., Lengeler, J.W., Jacobson, G.R., 1993. Phosphoenolpyruvate:carbohydrate phosphotransferase systems of bacteria. Microbiological Review 57, 543-594.

Restiawaty, E., Iwasa, Y., Maya, S., Honda, K., Omasa, T., Hirota, R., Kuroda, A., Ohtake, H., 2011. Feasibility of thermophilic adenosine triphosphate-regeneration system using *Thermus thermophilus* polyphosphate kinase. Process Biochemistry 46, 1747-1752.

Rohlin, L., Oh, M.K., Liao, J.C., 2001. Microbial pathway engineering for industrial processes: evolution, combinatorial biosynthesis and rational design. Current Opinion in Microbiology 4, 330-335.

Ruschig, U., Müller, U., Willnow, P., Höpner, T., 1976. CO_2 reduction to formate by NADH catalysed by formate ehydrogenase from *Pseudomonas oxalaticus.* European Journal of Biochemistry 70, 325-330.

Ryan, J.D., Fish, R.H., Clark, D.S., 2008. Engineering cytochrome P450 enzymes for improved activity towards biomimetic 1,4-NADH cofactors. ChemBioChem 9, 2579-2582.

Sato, M., Masuda, Y., Kirimura, K., Kino, K., 2007. Thermostable ATP regeneration system using polyphosphate kinase from *Thermosynechococcus elongatus* BP-1 for D-amino acid dipeptide synthesis. Journal of Bioscience and Bioengineering 103, 179-184.

Stephanopoulos, G., 2007. Challenges in engineering microbes for biofuels production. Science 315, 801-804.

Stephanopoulos, G., Sinskey, A.J., 1993. Metabolic engineering-methodologies and future prospects. Trends in Biotechnology 11, 392-396.

Tang, C.L., Hsu, R.Y., 1973. Reduction of α-oxo carboxyylic acids by pigeon liver malic enzyme. Biochemical Journal 135, 287-291.

Thauer, R.K., Jungermann, K., Decker, K., 1977. Energy conservation in chemotrophic anaerobic bacteria. Bacteriological Reviews 41, 100-180.

Tuesink, B., Passarge, J., Reijenga, C.A., Esgalhado, E., van der Weijden, C.C., Schepper, M., Walsh, M.C., Bakker, B.M., van Dam, K., Westerhoff, H.V., Snoep, J.L., 2000. Can yeast glycolysis be understood in terms of *in vitro* kinetics of the constituent enzymes? Testing biochemistry. European Journal of Biochemistry 267, 5313-5329.

Tuininga, J.E., Verhees, C.H., van der Oost, J., Kengen, S.W., Stams, A.J., de Vos, W.M., 1999. Molecular and biochemical characterization of the ADP-dependent phosphofructokinase from the hyperthermophilic archaeon *Pyrococcus furiosus*. The Journal of Biological Chemistry 274, 21023-21028.

Turner, P., Mamo, G., Karlsson, E.N., 2007. Potential and utilization of thermophiles and thermostable enzymes in biorefining. Microbial Cell Factories 6, 9.

Umbreit, W.W., Burris, R.H., Stauffer, J.F., 1957. Manometric Techniques, 3rd ed. Burgess Publishing Co., Minneapolis.

Valverde, F., Losada, M., Serrano, A., 1999. Engineering a central metabolic pathway: glycolysis with no net phosphorylation in an *Escherichia coli* gap mutant complemented with a plant *GapN* gene. FEBS Letters 449, 153-158.

Verhees, C.H., Kengen, S.W., Tuininga, J.E., Schut, G.J., Adams, M.W., de Vos, W.M., van der Oost, J., 2003. The unique features of glycolytic pathways in Archaea. Biochemical Journal 375, 231-246.

Wang, Y., Zhang, Y.H.P., 2009. Overexpression and simple purification of the *Thermotoga maritima* 6-phosphogluconate dehydrogenase in *Escherichia coli* and its application for NADPH regeneration. Microbial Cell Factories 8, 30.

Welch, P., Scopes, R.K., 1985. Studies on cell-free metabolism: Ethanol production by a yeast glycolytic system reconstituted from purified enzymes. Journal of Biotechnology 2, 257-273.

Werpy, T., Petersen, G., 2004. Top value added chemicals from biomass: Volume I: results of screening for potential candidates from sugars and synthesis gas. US Department of Energy.

Wichmann, R., Vasic-Racki, D., 2005. Cofactor regeneration at the lab scale. Advances in Biochemical Engineering/Biotechnology 92, 225-260.

Wintrode, P.L., Miyazaki, K., Arnold, F.H., 2001. Patterns of adaptation in a laboratory evolved thermophilic enzyme. Biochimica et Biophysica 1549, 1-8.

Wu, J.T., Wu, L.H., Knight, J.A., 1986. Stability of NADPH: effect of various factors on the kinetics of degradation. Clinical Chemistry 32, 314-319.

Xia, X., Qian, Z., Ki, C., Park, Y., Kaplan, D.L., Lee, S., 2010. Native-sized

recombinant spider silk protein produced in metabolically engineered *Escherichia coli* results in a strong fiber. Proceedings of the National Academy of Sciences 107, 14059-14063.

Yamaguchi, M., 1979. Studies on regulatory functions of malic enzymes. IV. Effects of sulfhydryl group modification on the catalytic function of NAD-linked malic enzyme from *Escherichia coli*. The Journal of Biochemistry 86, 325-333.

Yao, S., Mikkelsen, M.J., 2010. Metabolic engineering to improve ethanol production in *Thermoanaerobacter mathranii*. Applied Microbiology and Biotechnology 88, 199-208.

Ye, X., Honda, K., Sakai, T., Okano, K., Omasa, T., Hirota, R., Kuroda, A., Ohtake, H., 2012. Synthetic metabolic engineering- a novel, simple technology for designing a chimeric metabolic pathway. Microbial Cell Factories 11, 120.

Yokoyama, S., Matsuo, Y., Hirota, H., Kigawa, T., Shirouzu, M., Kuroda, Y., Kurumizaka, H., Kawaguchi, S., Ito, Y., Shibata, T., Kainosho, M., Nishimura, Y.,

Inoue, Y., Kuramitsu, S., 2000. Structural genomics projects in Japan. Nature Structural & Molecular Biology 7, 943-945.

Zelle, R.M., de Hulster, E., van Winden, W.A., de Waard, P., Dijkema, C., Winkler, A.A., Geertman, J.W., van Dijken, J.P., Pronk, J.T., van Maris, A.J., 2008. Malic Acid production by *Saccharomyces cerevisiae*: engineering of pyruvate carboxylation, oxaloacetate reduction, and malate export. Applied and Environmental Microbiology 74, 2766-2777.

Zelle, R.M., Harrison, J.C., Pronk, J.T., van Maris, A.J., 2011. Anaplerotic role for cytosolic malic enzyme in engineered *Saccharomyces cerevisiae* strains. Applied and Environmental Microbiology 77, 732-738.

Zhang, Y.H.P., 2010. Production of biocommodities and bioelectricity by cell-free synthetic enzymatic pathway biotransformations: challenges and opportunities. Biotechnology and Bioengineering 105, 663-677.

Zhang, Y.H.P., Evans, B.R., Mielenz, J.R., Hopkins, R.C., Adams, M.W.W., 2007.

High-yield hydrogen production from starch and water by a synthetic enzymatic pathway. PLos ONE 2, 456.

Zhang, Y.H.P., Sun, J., Zhong, J.J., 2010. Biofuel production by *in vitro* synthetic enzymatic pathway biotransformation. Current Opinion in Biotechnology 21, 663-669.

Zheng, H., Ohno, Y., Nakamori, T., Suye, S., 2009. Production of L-malic acid with fixation of HCO_3^- by malic enzyme-catalyzed reaction based on regeneration of coenzyme on electrode modified by layer-by-layer self-assembly method. Journal of Bioscience Bioengineering 107, 16-20.

RELATED PUBLICATIONS

Ye, X., Honda, K., Sakai, T., Okano, K., Omasa, T., Hirota, R., Kuroda, A., and Ohtake, H., 2012. Synthetic metabolic engineering- a novel, simple technology for designing a chimeric metabolic pathway. Microbial Cell Factories 11, 120.

Ye, X., Honda, K., Morimoto, Y., Okano, K., and Ohtake, H., 2013. Direct conversion of glucose to malate by synthetic metabolic engineering. Journal of Biotechnology (In press)

PRESENTATIONS IN CONFERENCES

Ye, X., Honda, K., Omasa, T., Ohtake, H.: Construction of chimeric glycolytic pathway by synthetic metabolic engineering. International Union of Microbiological Societies Congress (IUMS), 2011, September 6-10, Sapporo, Japan (Poster presentation)

Ye, X., Sakai, T., Okano, K., Hirota, R., Kuroda, A., Honda, K., and Ohtake, H.: Synthetic Metabolic Engineering-A novel, simple technology to design a chimeric metabolic pathway. Osaka Mini Symposium, 2012, March 12, Osaka, Japan (Oral presentation)

Ye, X., Sakai, T., Okano, K., Hirota, R., Kuroda, A., Honda, K., and Ohtake, H.: Construction of a chimeric glycolytic pathway for stoichiometrical production of lactic acid using thermophilic enzymes. Annual Meeting of Japan Society for Bioscience, Biotechnology and Agrochemistry, 2012, March 22-26, Kyoto, Japan (Oral presentation)

ACKNOWLEDGMENTS

It would not have been possible to write this doctoral thesis without the help and support of the kind people, to only some of whom it is possible to give particular mention here.

Above all, the author would like to express the sincere appreciation to Prof. Dr. Hisao Ohtake, who gives her the opportunity to conduct the M.S. and Ph.D. study in Osaka University. The author is in debt to Prof. Dr. Eiichiro Fukusaki and Prof. Dr. Toshiya Muranaka for their useful comments and suggestions to improve the thesis. This thesis would not have been possible without the help, support and patience of principal supervisor, Assoc. Prof. Dr. Kohsuke Honda, not to mention his advice, support on both academic and a personal level, for which she is extremely grateful. The author is also grateful to Prof. Dr. Takeshi Omasa from Tokushima University and Dr. Kenji Okano for their helpful advice and encouragements.

The author is grateful to Dr. Haruyuki Atomi from Kyoto University for kindly donating the *Thermococcus* GAPN expression vector. The author thanks Dr. Takashi Hirasawa from Osaka University for the CE-TOFMS analysis.

The author greatly appreciates all the members of Ohtake laboratory for their help, support and encouragement.